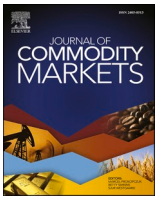
Journal of Commodity Markets 41 (2026) 100541



Contents lists available at ScienceDirect

Journal of Commodity Markets

journal homepage: www.elsevier.com/locate/jcomm



Regular article



# Renewable sources and short-to-mid-term electricity price forecasting

Niaz Bashiri Behmiri [a,b,*], Carlo Fezzi [c,d], Francesco Ravazzolo [e,f]

[a] Department of Business & Management Science, Norwegian School of Economics (NHH), Bergen, Norway
[b] Department of Business and Sustainability, SDU Climate Cluster, University of Southern Denmark, Esbjerg, Denmark
[c] Department of Economics and Management, University of Trento, Trento, Italy
[d] Land, Environment, Economics and Policy Institute (LEEP), Department of Economics, University of Exeter Business School, Exeter, United Kingdom
[e] Department of Data Science and Analytics, BI Norwegian Business School, and Faculty of Economics and Management Oslo, Norway
[f] Free University of Bozen-Bolzano, Bolzano, Italy

ARTICLE INFO

*Keywords:*
Mid-term electricity price forecasting
Renewable energy sources
Time series models

ABSTRACT

This study examines short-to mid-term point forecasting of daily electricity prices, with particular emphasis on the role of renewable energy sources. We use data from the market zone corresponding to the Northern region of Italy, applying both time series and machine learning methodologies. The forecasts are evaluated for two individual years, 2019 and 2024. In 2019, traditional energy variables such as electricity load, natural gas prices, and imports, were the primary drivers of forecast accuracy. During this period, adding renewable energy production data offered negligible benefits, with solar and wind contributing only marginally. By contrast, in 2024, market volatility increased greatly due to geopolitical conflicts and increased renewable energy integration. Under these conditions, while solar and wind still added limited value, hydropower improved forecast accuracy substantially. The results suggest that the role of renewable energy sources in electricity price forecasting is growing. However, their predictive power is influenced by their market share and by their variability and predictability.

## 1. Introduction

This study augments the existing literature on electricity price forecasting in the short- and mid-terms, with a particular focus on the impact of renewable energy sources. By integrating the dynamics of renewable energy production into the forecasting models, we shed light on their effects on price in the short and mid-term, i.e., from one-day to six-months ahead. This approach provides valuable insights for policymakers, stakeholders, and investors concerned with the future of sustainable energy markets.

The deregulation of electricity markets has transformed a formerly monopolistic sector into a competitive market structure. As a result, many countries now rely on spot and derivative contracts for electricity trading under established market rules (Weron, 2014). In liberalized markets, electricity is traded on wholesale exchanges through sequential day-ahead, intraday, and balancing markets (Gianfreda et al., 2020). The day-ahead market is central to electricity trading, as it shapes bidding behavior and market outcomes. Accurate day-ahead price forecasting is therefore essential for efficient market functioning, supporting optimal bidding strategies and

* Corresponding author. Department of Business & Management Science, Norwegian School of Economics (NHH), Bergen, Norway.
*E-mail addresses:* Bashiri.niaz@gmail.com (N.B. Behmiri), carlo.fezzi@unitn.it (C. Fezzi), francesco.ravazzolo@unibz.it (F. Ravazzolo).

https://doi.org/10.1016/j.jcomm.2026.100541
Received 11 August 2024; Received in revised form 10 January 2026; Accepted 20 January 2026
Available online 23 January 2026
2405-8513/© 2026 The Authors. Published by Elsevier B.V. This is an open access article under the CC BY license (http://creativecommons.org/licenses/by/4.0/).

effective risk management. Reliable forecasts allow market participants, including industrial consumers, generators, and utilities, to adjust bidding behavior and production or consumption plans accordingly. Beyond short-term horizons, mid-term price forecasting is also important for decisions related to maintenance planning, bilateral contracting, budgeting, risk management, and derivative pricing (Weron, 2014).

However, unlike other commodities, electricity exhibits several distinctive characteristics that complicate price prediction. Electricity is non-storable, and system stability therefore requires a continuous balance between production and consumption (Kaminski, 2013; Weron, 2014; Jiang et al., 2023). Furthermore, electricity demand is highly inelastic in the short-term (Fezzi and Bunn, 2010; Muniain and Ziel, 2020; Jiang et al., 2023). Consequently, electricity markets display pronounced price variability, demand-driven calendar seasonality, occasional and short-lived price spikes, nonlinearity, as well as non-linear and heteroscedastic behavior (Fezzi and Mosetti, 2020; Jiang et al., 2023). These features complicate the accurate forecasting of electricity prices.

To address these challenges, a large body of literature employs a wide range of methods and models to forecast electricity prices over both short-term horizons (e.g., Ciarreta et al., 2023; Jiang et al., 2023; Ghelasi and Ziel, 2023) and mid-term horizons (e.g., Busse and Rieck, 2022; Wagner et al., 2022). The performance of these methods depends on several factors, including the presence of volatility and price spikes within the forecast horizon. Consequently, there is no consensus on a definitive best practice for electricity price forecasting. This field of research continues to evolve, as market structures, participant behavior, and data-generating processes change over time. The recent innovations in energy production and especially the large increase in renewable energy resources, have added further complexity to electricity system management (Foroni et al., 2023). It is, therefore, essential to incorporate the impact of expanding renewable energy sources into price forecasting models.

One of the most significant impacts of increasing renewable sources is that it compels producers with higher-priced supply bids to lower their prices to remain competitive within the merit order (Antweiler and Muesgens, 2021). However, the impact of renewable energy sources on electricity prices varies according to multiple factors, such as market design, government policies, storage capacity, grid infrastructure, and regional resource availability. Consequently, the specific effects of renewable generation on electricity prices can differ significantly across regions and evolve over time. The interplay of these factors shapes the overall impact of renewable generation on price formation, making it a complex and dynamic relationship (IRENA,[1] 2019). This study forecasts short- and mid-term electricity prices by integrating both the supply and demand-side dynamics and evaluating the impact of renewable energy sources on forecasting performance.

Many previous studies that consider supply and demand in forecasting electricity prices focus on short-term horizons of a few days ahead, with several excluding renewable sources entirely from their analysis. (e.g., Nowotarski and Weron, 2016; Li and Becker, 2021). In contrast, a limited number of short-term forecasting studies incorporate the renewable generation (e.g., Gürtler and Paulsen, 2018; Gianfreda et al., 2020; Billé et al., 2023). These studies often rely on historical (actual) data as proxies for future values of input variables or combine forecasted and historical data. A minority of studies utilize forecasted values for all input variables, including renewable sources, to conduct short-term price forecasting (e.g., Gianfreda et al., 2020; Maciejowska et al., 2021; Lago et al., 2021; Wagner et al., 2022; Olivares et al., 2023; Uniejewski and Maciejowska, 2023).

In mid-term forecasting, variables such as load, renewable sources, and fuel prices, which are non-deterministic in nature, must also be forecasted. Given the complexity of this task, several studies conduct mid-term electricity price forecasting without incorporating explanatory variables that require future values estimation (e.g., Steinert and Ziel, 2019). Moreover, some studies employ actual values for both training and testing periods (e.g., Lehna et al., 2022), thereby bypassing the forecasting of input variables. Finally, a limited number of studies perform probabilistic forecasting beyond a one-month horizon using forecasted input variables rather than their actual values, while accounting for renewable energy sources (e.g., Ziel and Steinert, 2018).

Considering this background, the current literature reveals three primary limitations. First, there is a gap in mid-term point forecasting beyond a thirty-day horizon using daily data. Second, existing literature lacks an evaluation of the impact of incorporating forecasted exogenous variables for mid-term point forecasting, except for Ziel and Steinert (2018), who focus on probabilistic forecasts. Third, there is a lack of assessment regarding the predictive power of renewable energy sources within the context of daily and mid-term electricity price forecasts. This study aims to contribute to existing literature by addressing these three limitations. First, we conduct point forecasting for electricity prices across short-and-mid-term horizons, ranging from one-day to six-months ahead, utilizing daily data. We also ensure the robustness of our forecasts by substituting the actual values of exogenous inputs data with forecasted variables during the out-of-sample period. In doing so, we focus on assessing the predictive contribution of renewable energy sources. We compare models that incorporate hydroelectric power, onshore wind, and solar Photovoltaic (PV) generations against baseline specifications that exclude renewable sources.

We use daily data from the Northern Italy zone, spanning from July 2016 to December 2024. Northern Italy serves as an ideal case study for several reasons. First, it is the most industrialized region in Italy, with high electricity demand representing nearly half of the national total demand. This creates opportunities for strategic utilization of balancing sessions in response to supply and demand variations (Billé et al., 2023). Furthermore, this region has a distinct generation mix, with hydroelectric power historically playing an important role in meeting local demand. In recent years, wind and solar generation have also expanded in line with national and EU renewable energy targets. Finally, the region's interconnections with neighboring countries, including France, Switzerland, Austria, and Slovenia, make it a central part of the wider European electricity market.

These characteristics make Northern Italy an attractive case study for examining how renewable generation influences electricity

[1] International Renewable Energy Agency.

price dynamics in interconnected European sub-markets. Consequently, forecasting electricity prices in Northern Italy can improve understanding of the main drivers of price formation and shed light on potential outcomes as the share of renewable energy in the generation mix continues to increase. In this context, Shah and Lisi (2019), Bernardi and Lisi (2020), and Billé et al. (2023) use hourly data to forecast electricity prices in Northern Italy up to one day ahead; however, no study evaluates forecasts over longer horizons.

We develop several models, both with and without supply- and demand-side variables as inputs, using time-series and feed-forward neural network approaches for forecasting. The forecasts are evaluated for two distinct years: 2019, when the renewable sources were still limited, and 2024, when the share of renewable sources had increased. We find that in 2019, electricity load, natural gas prices, and imports played a dominant role in forecast accuracy. In contrast, renewable generation data offered limited benefits, with solar and wind contributing only marginally. In 2024, market volatility increased mainly due to geopolitical tensions, and the growing integration of renewable sources. In this context, solar and wind continued to offer limited predictive value, while hydropower emerged as a more informative input, improving forecasting accuracy.

The remainder of the paper is structured as follows. Section 2 provides a literature review. Section 3 describes Northern Italy electricity market structure. Section 4 introduces data. Section 5 explains the models and methods. Section 6 presents forecasting strategy, results and discussion. Finally, Section 7 concludes.

## 2. Electricity price forecasting literature

The literature on electricity price forecasting can be categorized based on various criteria, one of which is the forecast horizon. Some studies concentrate on short-term forecasts spanning from an hour to a few days ahead, including Fezzi and Mosetti (2020), Shao et al. (2022), Shi et al. (2021), Ghelasi and Ziel (2023), Ciarreta et al. (2023), and Jiang et al. (2023). Other studies examine mid-term forecasts ranging from a few weeks to several months ahead, such as Haugom and Ullrich (2012), Bigerna (2018), Steinert and Ziel (2019), Busse and Rieck (2022), Lehna et al. (2022), and Wagner et al. (2022). Finally, some contributions tackle long-term forecasts extending several years into the future, including Ziel and Steinert (2018).

Furthermore, this literature can be classified based on forecasting methods employed. Some studies use statistical, time series, and econometric methods, including Weron and Misiorek (2008), Escribano et al. (2011), Maciejowska et al. (2016), Ziel and Steinert (2018), Uniejewski et al. (2019), Gianfreda et al. (2020), Billé et al. (2023), Monjazeb et al. (2024) and Ghelasi and Ziel (2025). Other studies apply machine learning methods, such as Marcjasz et al. (2019), Olivares et al. (2023), and Belenguer et al. (2025), while hybrid methods are utilized by Yang et al. (2017) and Cheng et al. (2019), among others.

The literature predominantly focuses on short-term electricity price forecasting up to a few days ahead, often excluding information on renewable energy sources (e.g., Nowotarski and Weron, 2016; Li and Becker, 2021; Ciarreta et al., 2023; Jiang et al., 2023). Some studies incorporate renewable energy sources in short-term forecasting while assume future values of exogenous variables to be known, using either actual data or a combination of forecasted and actual data (e.g., Escribano et al., 2011; Gürtler and Paulsen, 2018; Gianfreda et al., 2020; Billé et al., 2023, Gianfreda et al., 2023). Other studies rely exclusively on forecasted values for all exogenous variables in short-term price forecasting (e.g., Maciejowska et al., 2021; Lago et al., 2021; Olivares et al., 2023; Uniejewski and Maciejowska, 2023).

Within this literature, some studies aim to forecast prices beyond the short-term horizon while incorporating exogenous variables. However, these studies typically treat future values of the explanatory variables as known and reply on actual data when forecasting up-to-one month ahead (Bigerna, 2018; Lehna et al., 2022; Foroni et al., 2023). In this context, limited studies extend price forecasts beyond a one-month horizon. For instance, Wagner et al. (2022) employ time series models and various neural network methodologies on hourly data. They forecast the 24-hourly prices for the following day by incorporating forecasted wind and solar PV as exogenous variables. Additionally, they extend their forecasting horizon to one-year by utilizing multiple sets of dummy variables and sinusoidal functions as exogenous variables. Consequently, the authors exclude the renewables generation variables from their mid- and long-term forecasting models. Among the existing studies, Ziel and Steinert (2018) stand out as the only study that conducts mid- and long-term forecasting while considering renewable sources and employing forecasted exogenous variables rather than the actual data. Their study applies hourly data and considers forecasting horizons of up to three years. The authors develop supply and demand curve-based models and employ lasso estimation techniques. Notably, they forecast wind, solar, and conventional generations for up to three-years ahead, which are subsequently incorporated into their price forecasting models. However, their focus is on probabilistic rather than point forecasts.

## 3. Northern Italy electricity market structure

Our empirical study focuses on the Northern Italy electricity zonal market. The Italian electricity market is organized into geographical and foreign virtual zones, which are designated areas within the national grid, marked by transmission capacity constraints. These zones involve six bidding zones: North, Central-North, Central-South, South, Sicily, and Sardinia.

Italy has made progress in market liberalization and development of infrastructure (IEA,[2] 2016). In Italy, the share of renewable energy has experienced remarkable growth, increasing from 14 % in 2005 to 35 % in 2018–2019 and reaching 41 % in 2024 (Terna).[3]. Despite the notable expansion, fossil fuels continue to dominate the electricity generation mix. In 2024, natural gas accounted for 45 %

[2] International Energy Agency.
[3] https://www.terna.it/en

of electricity output, followed by coal (9 %), biomass (9 %), and other fossil fuels (6 %), while renewables together supplied approximately 41 %. Among renewables, hydropower contributed approximately 16 %, solar power 12 %, and wind power around 6.5 %, with the remaining share coming from bioenergy and other minor renewable sources (IEA).

Accounting for approximately 45 %–50 % of Italy's total electricity consumption, Northern Italy represents a key regional market and is therefore highly relevant for electricity price forecasting studies. At the European level, Italy's electricity generation represented about 10 % of the EU total generation, ranking it as the fourth-largest electricity consumer after Germany, France, and Spain (Eurostat).[4]. Furthermore, Northern Italy has been historically distinguished by substantial hydroelectric power contributions and, in recent years, it has experienced a notable increase in solar PV penetration (Gianfreda et al., 2018). According to Terna's general data, most power plants in Italy are located along the Alps and more than 50 % of the country's total hydropower is generated in the Northern region. These information exhibit that Northern Italy plays a central role in the national electricity system and contributes significantly to the broader European electricity market as well. Consequently, improvements in forecasting accuracy for this region have both national and continental relevance.

In Italy, the Gestore dei Mercati Energetici (GME) acts as the central counterparty for the day-ahead market, operating as the central platform for electricity transactions conducted through auctions. The Gestore dei Servizi Energetici (GSE) is responsible for selling renewable energy production on the day-ahead market under a priority dispatch regime. Once solar and wind generation are fully dispatched, the remaining demand is met through competition among conventional generation units. Consequently, hourly prices are determined by the intersection of aggregated supply and demand curves and are influenced by the merit-order effect (Gianfreda et al., 2018). In this region, hydropower generation constitutes a strategic asset for both baseload and peak-load generation, contributing to system stability and market balance (Bonato et al., 2019).

## 4. Data

The daily electricity price in the North bidding zone is determined on the Italian Power Exchange (IPEX) day-ahead market and serves as the basis for the purchasing cost for end customers.

We downloaded hourly day-ahead price data from the GME. These prices are quoted in euros per Megawatt-hour (€/MWh) and are adjusted to account for daylight saving time changes, such as excluding the 25th hour in October and incorporating the missing 24th hour in March. We convert the hourly prices into daily prices by calculating their arithmetic average.

We consider both demand- and supply-side factors as determinants of electricity prices. To approximate the demand side, we utilize the actual daily load in the North bidding zone traded on the IPEX. We obtain the hourly day-ahead load data, measured in megawatt-hours (MWh) from the European Network of Transmission System Operators for Electricity (ENTSO-E). We convert the hourly load data into daily load by calculating their averages. As commonly assumed in the electricity price forecasting literature we treat demand as completely inelastic and model the traded quantity as exogenous (Nowotarski and Weron, 2016; Fezzi and Bunn, 2010). In addition to the actual load data, we require the forecasted load values for further analysis of ex-ante forecasts. In this context, air temperature plays a key role in load forecasting (Behm et al., 2020; Behmiri et al., 2023), and therefore to forecast load, we consider daily average temperature in Milan as the main explanatory variable. We collect daily temperature data from the Visual Crossing Website.

Supply is derived from a combination of fossil fuels, renewable sources, and imports. Fossil fuel prices enable us to capture the marginal cost associated with conventional thermal generation (Gianfreda et al., 2020). We retrieve daily settlement prices for natural gas from the Refinitiv Datastream database. We focus on Dutch TTF natural gas front-month contracts, quoted in euros per MMBtu[5] (€/MMBtu). Since this commodity is not traded during weekends and holidays, we employ a linear interpolation method to fill these gaps. As part of our representation of the supply curve, we include the contribution of renewable energy sources (RES). This encompasses onshore wind, solar PV, and the aggregate of various forms of hydroelectric power generation, namely hydro-pumped-storage, hydro-run-of-river and poundage, and hydro-water-reservoir. We collect hourly values for RES in MWh from the ENTSO-E and convert them into daily values by calculating their average.

To account for electricity transfers between bordering markets and neighboring bidding zones, we follow Billé et al. (2023) by calculating the weighted import price. This variable involves the daily average of day-ahead prices in foreign countries and neighboring zones weighted by the daily average of actual physical flows for that day. Accounting for price dynamics in neighboring zones and countries is critical, especially when their local energy mixes exhibit significant differences. Therefore, we reflect their distinct generation portfolios while applying price weights based on the imported quantities. Mathematically, this relationship can be represented as follows:

$$(\textit{Weighted import price})_t = \frac{\sum_{i=1}^{n} (p_{i,t} \times x_{i,t})}{\sum_{i=1}^{n} x_{i,t}}$$

where $p_{i,t}$ denotes the daily day-ahead prices observed in foreign countries and neighboring zones, measured in €/MWh, $x_{i,t}$ represents the quantity of electricity imported from each of these markets, measured in MWh, at a given time point $t$, and $i$ comprises Austria,

[4] https://ec.europa.eu/eurostat

[5] 1,000,000 British thermal units.

**Table 1**
Summary statistics.

| 06/07/2016-31/12/2024 | Unit | Mean | SD | Min | Max | Correlation with price | Sources |
|---|---|---|---|---|---|---|---|
| Electricity price | €/MWh | 105.56 | 96.86 | 10.70 | 751.29 | – | https://www.entsoe.eu/ |
| Load | MWh | 18238.43 | 3268.32 | 9266.75 | 26255.17 | 0.103[a] | https://www.entsoe.eu/ |
| Weighted import price | €/MWh | 89.58 | 91.37 | −3.45 | 732.75 | 0.979[a] | https://www.entsoe.eu/ |
| Natural gas price | €/MMBtu | 38.43 | 42.32 | 3.51 | 339.20 | 0.963[a] | https://solutions.refinitiv.com/ |
| Hydro generation | MWh | 3990.57 | 1724.63 | 804.79 | 9149.38 | −0.238[a] | https://www.entsoe.eu/ |
| Solar PV generation | MWh | 851.29 | 483.75 | 23.71 | 3031.54 | 0.028 | https://www.entsoe.eu/ |
| Wind generation | MWh | 22.18 | 26.49 | 0.17 | 156.08 | 0.148[a] | https://www.entsoe.eu/ |
| Temperature | °Fahrenheit | 58.48 | 14.67 | 27.00 | 87.00 | – | Weather Query Builder \| Visual Crossing |

Notes.
[a] indicates statistical significance at the 1 % level and SD represents the standard deviation.

France, Switzerland, Slovenia, and Central-Northern Italy. We obtain hourly data for imports and foreign prices from the ENTSO-E and convert them into daily values by calculating their average.

Our data cover the period from July 6, 2016, to December 31, 2024, yielding 3101 daily observations. Table 1 provides summary statistics, Pearson correlation coefficients between prices and input variables, and links to data sources. Electricity prices are positively and significantly correlated at the 1 % level with load, weighted import price, and natural gas price, while its correlations with renewable energy sources (RES) are mixed.

Fig. 1 illustrates the variation in electricity prices from July 6, 2016, to December 31, 2024. From 2016 until 2020, prices remained relatively stable, characterized by minor spikes. A pronounced upward trend began in mid-2021, leading to extreme volatility and price peaks in late 2021 and the first half of 2022. These spikes coincide with the European energy crisis, geopolitical tensions and natural gas supply shocks. Following this peak, prices declined in late 2022 but continued to fluctuate throughout 2023. By 2024, prices had stabilized, though they remained above pre-crisis levels.

Figs. 2–7 present scatterplots illustrating the relationship between electricity prices and the input variables. Fig. 2 shows that as load increases, prices tend to rise. This relationship becomes more pronounced when load reaches higher levels. Fig. 3 illustrates a strong positive correlation between the weighted import price and the Northern Italy price. This is expected, as the weighted import price is constructed by assigning weights to prices from foreign countries and neighboring zones based on actual physical flows. Fig. 4 illustrates a positive correlation between natural gas and electricity prices, confirming natural gas as the dominant fossil fuel in the Northern Italy's generation mix.

Figs. 5 and 6 illustrate a negative relationship between electricity prices and both hydropower and wind generation. This downward pressure on prices is particularly evident at higher levels of generation, consistent with the merit-order effect. Fig. 7 shows a similar negative relationship for solar PV, though the pattern is weaker compared to the correlations observed for hydropower and wind.

## 5. Models and methods

### 5.1. Linear regression forecasting models

We initiate our analysis by employing a set of benchmark time series methods: a) the naïve method, b) the autoregressive (*AR*)

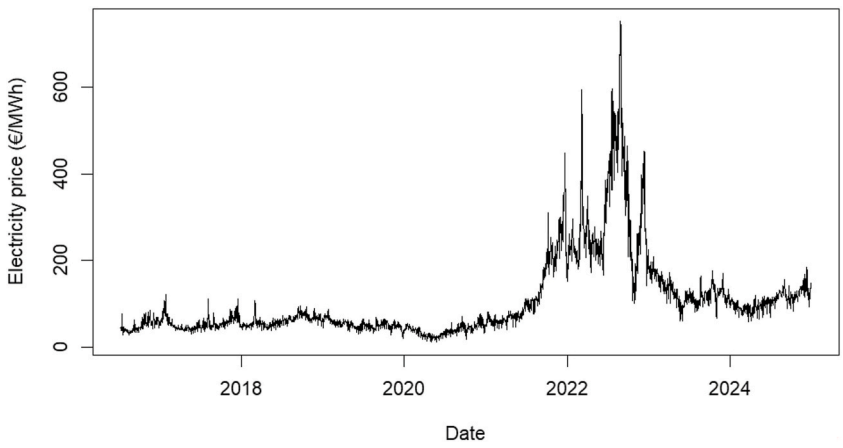



**Fig. 1.** Electricity price.

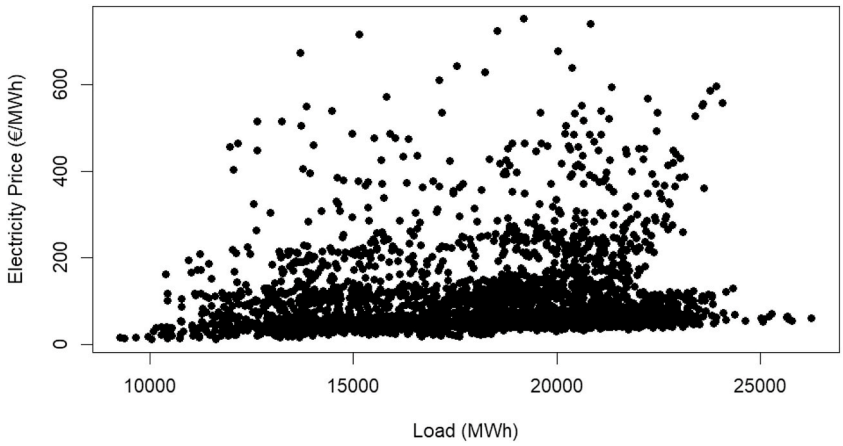



**Fig. 2.** Electricity price versus load.

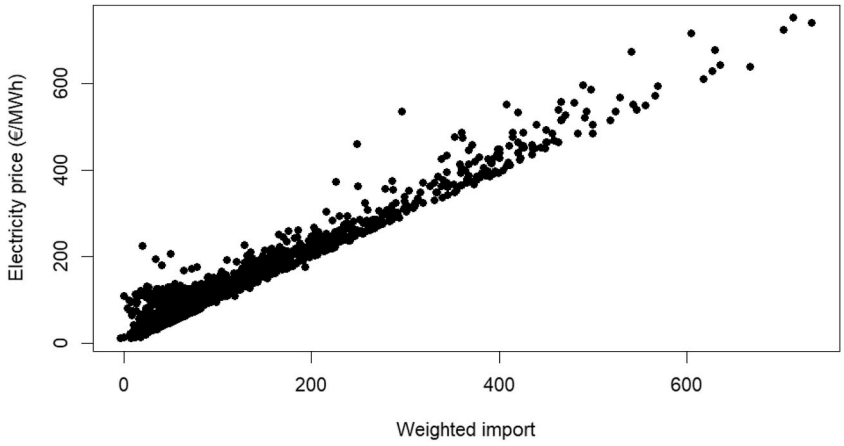



**Fig. 3.** Electricity price versus weighted import price.

model, and c) the Holt-Winters (H-W) approach (Holt, 1957; Winters, 1960). For the naïve method, the forecast is set equal to the last observation in the training sample. We estimate an $AR(7)$ model to capture weekly dependencies. Additionally, we employ the additive Holt-Winters method, assuming that weekly seasonal variations remain stable throughout the series.

Next, we develop a series of autoregressive models with exogenous inputs, expanding in a stepwise fashion. Gradually incorporating these drivers enables us to evaluate the predictive power of each variable in a systematic manner. Comparing these nested models allows us to determine the marginal contribution of RES variables to price forecasting accuracy. Model 1 incorporates load and past prices observed over a one-to-seven-day period, as follows:

$$y_t = \beta_0 + \sum_{i=1}^{7} \phi_i y_{t-7} + \beta_1 l_t + \varepsilon_t \tag{1}$$

where $y_t$ represents electricity price at time $t$, $l_t$ denotes electricity load at time $t$, $\beta_s$ and $\phi_i$ are parameters to be estimated, and $\varepsilon_t$ denotes the error term assumed to be white noise. By comparing Model 1 with the $AR(7)$, we gain insights into the contribution of load as a predictor of price dynamics.

In the next specification, we expand Model 1 by incorporating natural gas prices and the weighted import price. Model 2 is defined as follows:

$$y_t = \beta_0 + \sum_{i=1}^{7} \phi_i y_{t-7} + \beta_1 l_t + \boldsymbol{X_t}'\boldsymbol{\beta} + \varepsilon_t \tag{2}$$

where $\boldsymbol{X_t}'$ is a vector containing the weighted import prices and the natural gas prices at time $t$. All other variables are defined as

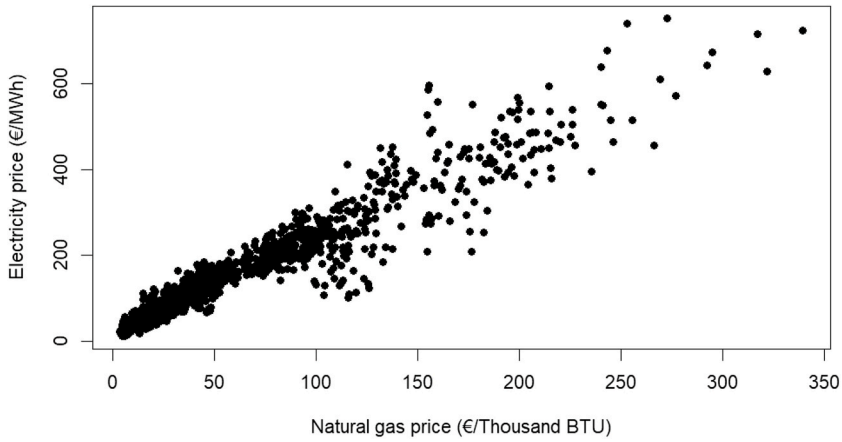



**Fig. 4.** Electricity price versus natural gas price.

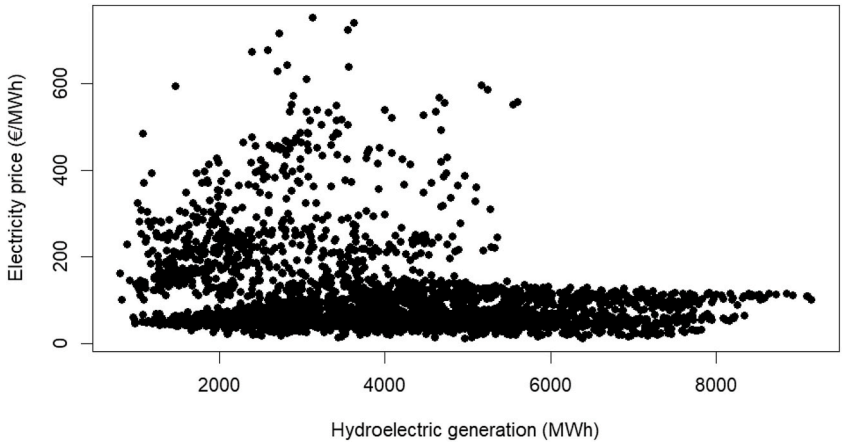



**Fig. 5.** Electricity price versus hydroelectric generation.

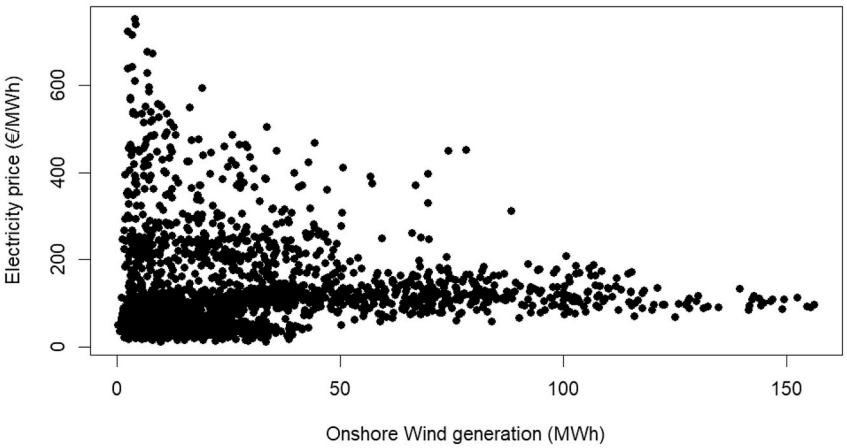



**Fig. 6.** Electricity price versus onshore wind generation.

previously. A comparative analysis between Model 2 and Model 1 reveals the role of natural gas and the weighted import prices in enhancing the accuracy of electricity price forecasts.

In the subsequent steps, our focus shifts to evaluating the effectiveness of RES in electricity price forecasting. Consequently, we extend Model 2 by sequentially incorporating RES variables in Models 3–5, defined as follows:

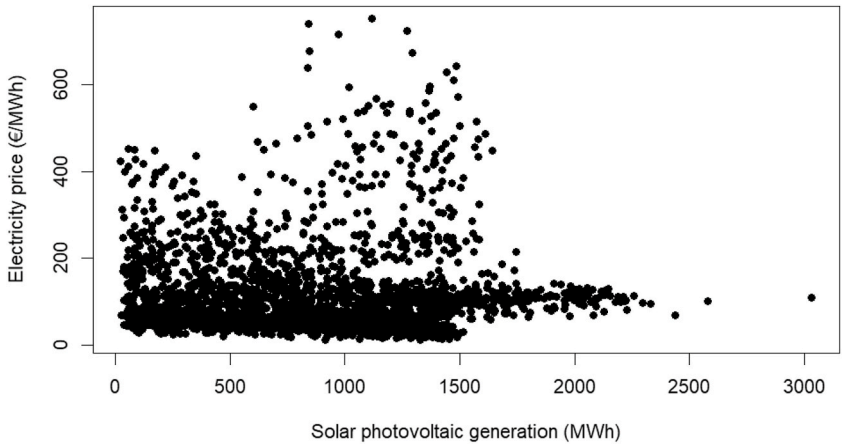



**Fig. 7.** Electricity price versus solar photovoltaic generation.

$$y_t = \beta_0 + \sum_{i=1}^{7} \phi_i y_{t-7} + \beta_1 l_t + \boldsymbol{X_t}'\boldsymbol{\beta} + \theta RES_t + \varepsilon_t \tag{3–5}$$

where $RES_t$ represents hydroelectric, solar PV, and wind generation at time $t$ in Models 3, 4 and 5, respectively, $\theta$ is the parameter to be estimated, and all other variables and symbols are defined as before. We also performed forecasts by integrating all three RES variables into a single model. However, this specification showed lower accuracy compared to the models where each RES type was included separately.

Electricity load presents calendar seasonality as demand is higher on working days than on weekends; moreover, yearly seasonality shows a peak in load during the winter (January and February) and summer (June, July, and August) due to cooling and heating requirements (Behmiri et al., 2023). Similarly, recurring patterns are observed in RES generation throughout the year, primarily influenced by weather conditions, solar irradiance, wind speeds, and water availability. These factors play a significant role in shaping the long-term price profile. While our initial assumption was that input variables incorporated in Models 1-5 adequately capture these trends, we now augment our analysis by introducing two new components: Fourier series (sinusoidal terms) to capture weekly seasonality, and monthly dummy variables to account for yearly fluctuations.

It is common practice to include Fourier terms of various frequencies to capture seasonal patterns (Wagner et al., 2022). We initially employed a combination of sine and cosine functions to approximate periodic variations, accounting for both weekly and monthly cycles. However, we found that incorporating weekly cycles alone, alongside monthly dummy variables, resulted in a better fit compared to models that incorporated both annual and weekly Fourier cycles. We define the Fourier terms as:

$$F = \sum_{k=1}^{K} \left( \tau_k \cos\left(\frac{2\pi k t}{L}\right) + \omega_k \sin\left(\frac{2\pi k t}{L}\right) \right)$$

We selected the optimal order for the Fourier series ($k = 3$) based on the model's performance. We began with $k = 1$, then we increased the order until the forecast errors no longer decreased. Moreover, $L = 7$ represents the seasonal period for the weekly pattern, and $\tau_k$, $\omega_k$ are parameters to be estimated. We extend Models 1–5 by adding the Fourier terms, monthly dummy variables, and time trend, resulting in Models 6–10. Model 6 extends Model 1 and is specified as follows:

$$y_t = \beta_0 + \sum_{i=1}^{7} \phi_i y_{t-7} + \beta_1 l_t + F + \boldsymbol{M_t}'\boldsymbol{\gamma} + \delta T_t + \varepsilon_t \tag{6}$$

where $F$ includes the Fourier terms, $\boldsymbol{M_t}'$ represents a set of five dummy variables for January, February, June, July, and August,[6] $T_t$ is the linear time trend, and $\gamma$ and $\delta$ are parameters to be estimated. All other variables and symbols are defined as before.

Expanding on Model 2, we introduce Model 7 with the same additional variables:

$$y_t = \beta_0 + \sum_{i=1}^{7} \phi_i y_{t-7} + \beta_1 l_t + \boldsymbol{X_t}'\boldsymbol{\beta} + F + \boldsymbol{M_t}'\boldsymbol{\gamma} + \delta T_t + \varepsilon_t \tag{7}$$

Following the same rationale, Models 8–10 are extensions of Models 3–5, respectively:

[6] We also incorporated eleven monthly dummy variables accounting for each month of the year; however, we find less accurate forecasts.

$$y_t = \beta_0 + \sum_{i=1}^{7} \phi_i y_{t-7} + \beta_1 l_t + \boldsymbol{X_t}'\boldsymbol{\beta} + \theta RES_t + F + \boldsymbol{M_t}'\boldsymbol{\gamma} + \delta T_t + \varepsilon_t \quad (8\text{–}10)$$

All variables and symbols in Models 6–10 are defined previously. We conduct in-sample estimations using the Maximum Likelihood (ML) estimation method.

### 5.2. Neural network forecasting

We also evaluate the forecasting performance of Artificial Neural Networks (*ANNs*). We use the multilayer feed-forward neural network (*FFNN*) approach, a type of *ANN* consisting of input, hidden, and output layers. The *FFNN* is an established type of *ANN* in the electricity price forecasting literature (e.g., Catalao et al., 2007; Poggi et al., 2023).

In the FFNN approach, information flows only from the input nodes through the hidden nodes to the output nodes (Andreas, 1994). The input layer receives the data and sends it to the hidden layer via the weights between the input and hidden layers. The hidden layer processes the data and forwards it to the output layer using the weights between the hidden and output layers. The neurons in the output layer then process the data again and produce the results as the output (Engelbrecht, 2007). The *FFNN* can be mathematically represented as:

In the *FFNN* approach information flows only from the input nodes through the hidden nodes to the output nodes (Andreas, 1994). The input layer receives the data and sends it to the hidden layer via the weights between the input and hidden layers. The hidden layer processes the data and forwards it to the output layer, using the weights between the hidden and the output layers. The neurons in the output layer then processes the data again and produces the results as the output (Engelbrecht, 2007). The *FFNN* can be mathematically represented as:

$$y_t = f\left(b + \sum_{j=1}^{h} v_j\, g\left(b_j + \sum_{i=1}^{n} w_{ij} X\right)\right),$$

where $y_t$ is the output variable at time $t$, $X$ represents a vector of input variables and the lagged output variable, and $h$ and $n$ denote the number of neurons in the hidden layer defined as half of the number of input variables plus one, and the number of input variables, respectively. The terms $f(.) = \frac{1}{1+exp^{-f}}$ and $g(.) = \frac{1}{1+exp^{-g}}$ are the sigmoid non-linear activation functions. Furthermore, $v_j$ and $w_{ij}$ are the weight parameters representing the strength of the connections between the hidden nodes and the output and between the input nodes and the hidden nodes, respectively (Sulandari et al., 2020). Finally, $b$ and $b_j$ are the bias parameters equivalent to the intercept. All parameters are estimated using the BFGS[7] optimization algorithm (Fletcher, 1987).

## 6. Forecasting strategy, results and discussion

### 6.1. Forecasting strategy

We use the observed values of the input variables to forecast price, assuming that these variables are known over the forecast horizon. Model selection is based on forecast errors, which guide the choice of the appropriate specification, autoregressive order, and the number of Fourier terms. The forecasting horizons considered include one to seven days ahead, fourteen days ahead, and one to six months ahead (corresponding to 30–180 days).

To ensure the robustness and generalizability of our findings, we first evaluate the models' performance using an aggregate out-of-sample forecasting framework spanning from 2019 through 2024. This multi-year aggregation validates the structural stability of our proposed models and provides a rigorous assessment of their capacity to account for long-term temporal trends across diverse market regimes. By reporting average performance metrics over this extended period, we demonstrate that our results are not skewed by the idiosyncratic volatility of any single year but rather reflect a consistent predictive superiority over the benchmark. To examine the impact of changes in the renewable energy mix, we extend the analysis by comparing two representative years of 2019 and 2024. This comparative approach allows us to isolate the effects of increased intermittent generation and evolving market penetration of renewables by distinguishing between a pre-crisis and the current state of the energy system.

We split the daily dataset into two segments for in-sample estimation and out-of-sample forecasting. The forecast for each year starts on January 1 and ends on December 31. For estimation, we use rolling windows of size set at two years (730 days), i.e. the estimation window length remains constant across all forecasting dates and horizons. The window for estimation begins from the date $t^* - 730 - J$ and extends to the date $t^* - J$, where $t^*$ represents the target date for out-of-sample forecasting and $J$ denotes the forecasting horizon (e.g., $J = 1$ for day-ahead forecasts, $J = 2$ for two-days ahead forecasts, $J = 180$ for six-months forecast and so forth).

As an example, suppose the target forecast date is January 1, 2019, for all forecast horizons. For a one-day-ahead forecast ($J = 1$), the estimation window spans from January 1, 2017, to December 31, 2018. For a two-day-ahead forecast ($J = 2$), the estimation window runs from December 31, 2016, to December 30, 2018. For a six-months ahead forecast ($J = 180$), the estimation window covers the period from July 6, 2016, to July 4, 2018. For forecasting horizons longer than one day, all models use the forecast from the

[7] Broyden, Fletcher, Goldfarb, and Shanno.

previous step as an input for the next step; that is, we employ recursive multi-step-ahead forecasting.

We evaluate forecast performance using Root Mean Square Error (RMSE) and Mean Absolute Percentage Error (MAPE). The RMSE is computed using the following formula:

$$\mathrm{RMSE_k} = \sqrt{\frac{\sum_{t=1}^{N}\left(\widehat{y}_{t,k} - y_t\right)^2}{N}}$$

Moreover, the MAPE is calculated as:

$$\mathrm{MAPE_(k)} = \left(1 \Big/ \mathrm{N}\sum_{t=1}^{N}\left|\frac{y_t - \widehat{y}_{t,k}}{y_t}\right|\right) \times 100$$

where $N$ is the number of observations in the forecasting window, $y_t$ is electricity price at time $t$, and $\widehat{y}_{t,k}$ is the forecasted price at time $t$ by model $k$. Furthermore, using the Diebold and Mariano (1995) test, we assess the performance of the models by comparing them to the benchmark model.

The analyses are conducted within the statistical software R (R Core Team, 2021), using the *forecast* (Hyndman et al., 2020) and *psych* (Revelle, 2016) packages.

### 6.2. Results and discussion

This section evaluates the out-of-sample performance of the suggested models in forecasting daily electricity prices across different horizons. We began by analyzing horizon-specific performance through the aggregation of RMSE and MAPE for out-of-sample forecasts spanning the 2019–2024 period. Figs. 8 and 9 illustrate the comparative forecasting performance of ten econometric models, the naive, and the Holt-Winters models, against the Benchmark *AR*(7), across one-day to six-months forecast horizons for the aggregate period of 2019–2024. The output is illustrated in Figs. 8–9. By averaging these metrics across a five-year window that includes various market cycles, we provide a robust assessment of the models' stability and predictive accuracy across horizons ranging from one-day to six-months.

Figs. 8–9 illustrate that forecasting error increases as the time horizon extends from one-day (1D) to six-months (6M); however, they also reveal a significant variation in model reliability. Models 1 and 6, which only include load, underperform the benchmark; however, all the other models consistently outperform the benchmark. Models 4, 5, and 10 (including solar and wind generation) appear as the best performers, consistently maintaining the lowest error rates (MAPE under 20 % and RMSE below 50) throughout the entire forecast horizons.

When the analysis is conducted separately for each year from 2019 to 2024, there is evidence that our suggested models consistently outperform the benchmark. To conserve space, these year-by-year results are not reported. However, we extend the analysis by

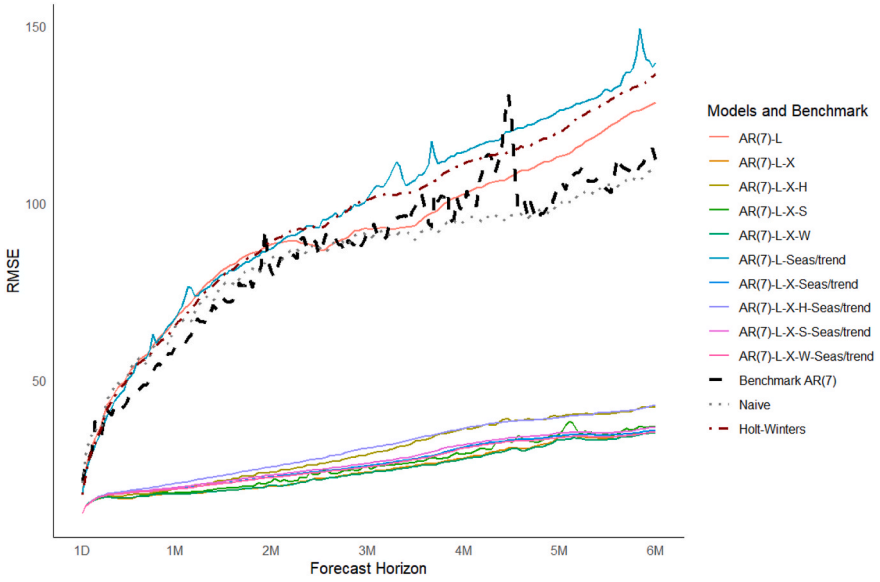



**Fig. 8.** RMSEs comparison of time series models for aggregated period 2019–2024.
Note: The variable L denotes load; X includes the weighted import price and natural gas price; and H, S, and W represent hydroelectric, solar PV, and onshore wind generation, respectively. The term *"Seas/trend"* refers to models incorporating Fourier terms, monthly dummy variables, and a linear time trend.

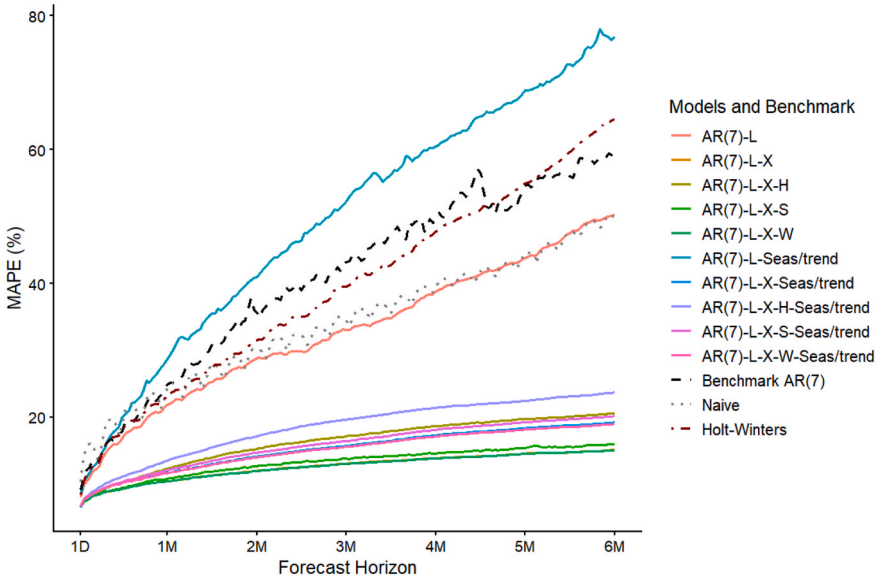



**Fig. 9.** MAPEs comparison of time series models for aggregated period 2019–2024.
Note: The variable L denotes load; X includes the weighted import price and natural gas price; and H, S, and W represent hydroelectric, solar PV, and onshore wind generation, respectively. The term *"Seas/trend"* refers to models incorporating Fourier terms, monthly dummy variables, and a linear time trend.

reporting the results for the year 2019 and the year 2024 in more detail to shed light on the evolution of the predictive power of renewable energy sources.

The evaluation is extended by comparing two representative years of 2019 and 2024, using the RMSE in Tables 2 and 3, and the MAPE in Tables 4 and 5. All tables are divided into two sections. The first section presents the results from time series models (referred to as Time Series), and the second section shows the results from feed-forward neural networks (referred to as *FFNN*).

Each section is further divided into two panels, labeled Panel A and Panel B. In the time series models section, Panel A includes the outputs from the Naïve, the Holt-Winters, and an autoregressive model with 7 lags (*AR*(7)), and Panel B reports the results from Models 1 through 10, which incorporates exogenous input variables. In the feed-forward neural networks section, Panel A contains the Naïve model and a feed-forward neural network autoregressive model with 7 lags, 10 hidden units, and 5 repeats (denoted as *FFNNAR*(7, 10, 5)). Panel B presents the results from Models 1 through 10, employing the same *FFNNAR* architecture but incorporating input variables.

In all tables, the values in bold represent the lowest RMSE or MAPE for each time horizon within each panel, while the values highlighted in grey indicate the models with the highest accuracy for each time horizon across all models. For instance, when using time series models for the year 2019, for the one-day to one-month forecast horizons, the Holt-Winters model exhibits the best performance amongst time series models in Panel A. However, for longer horizons, the *AR*(7) model outperforms the other two time series methods reported in Panel A. The smallest RMSE in this panel (4.77 €/MWh) corresponds to the one-day ahead forecast, while the largest value is for the six-months ahead forecast (11.84 €/MWh).

We conduct the Diebold-Mariano test for all Models 1 through 10 to assess their forecasting performance. For the time series models, each model is compared against the benchmark *AR*(7), while for the *FFNN* models, the comparison is made against the *FFNNAR*(7, 10, 5) benchmark. As a general conclusion, the test outputs reveal that, at the 1 %, 5 %, and 10 % levels of significance, there are several models across all forecast horizons that significantly outperform the benchmark models, confirming the relevance of the input variables. In the following paragraphs we elaborate on these results in more detail.

### *6.2.1. Year 2019*

Starting with the year 2019, as reported in the first section of Table 2 (*Time Series*), the results suggest that adding load data (Model 1) improves the forecast accuracy of the *AR*(7) model. The RMSE drops by an average of 13 %–33 % across horizons, with the most significant gains at short-term horizons (e.g., from 5.38 to 3.97 for the one-day ahead forecast). By introducing natural gas prices and weighted imports (Model 2), we find further improvements in accuracy. Compared to Model 1, the RMSE drops by an average of 1 %–38 % across forecast horizons, specifically improving performance at the medium-term horizons.

Models 3, 4, and 5 extend Model 2 by incorporating renewable generation sources: hydropower, solar, and wind, respectively. In the case of 2019, the inclusion of hydropower in Model 3 leads to a deterioration in forecast performance, with RMSE values increasing by 3 %–55 % compared to Model 2. The most pronounced increase occurs at longer-term horizons, suggesting that hydropower data does not contribute to predicting prices during this period.

Models 4 and 5, which include solar and wind generation respectively, exhibit only marginal improvements. Model 4 realizes slight

**Table 2**
RMSE for ex-post forecasts of electricity prices in 2019.

| TimeSeries | 1D | 2D | 3D | 4D | 5D | 6D | 7D | 14D | 1M | 2M | 3M | 4M | 5M | 6M |
|---|---|---|---|---|---|---|---|---|---|---|---|---|---|---|
| **Panel A: No Input Variables** | | | | | | | | | | | | | | |
| Naive | 6.32 | 8.65 | 9.35 | 9.69 | 9.38 | 8.35 | 7.51 | 9.21 | 11.66 | 11.98 | 12.37 | 14.30 | 16.63 | 17.30 |
| Holt-Winters | **4.77** | **5.70** | **6.06** | **6.53** | **6.74** | **7.01** | **7.23** | **8.81** | **9.71** | 10.80 | 13.73 | 17.22 | 19.96 | 22.66 |
| AR(7) | 5.38 | 6.58 | 6.89 | 7.12 | 7.22 | 7.25 | 7.40 | 8.96 | 9.87 | **10.43** | **10.81** | **11.33** | **11.83** | **11.84** |
| **Panel B: With Actual Input Variables** | | | | | | | | | | | | | | |
| Model 1: AR(7)-L | 3.97*** | 4.45*** | 4.60*** | 4.86*** | 5.05*** | 5.26*** | 5.37*** | 6.44*** | 7.99*** | 9.06*** | 9.24*** | 9.65*** | 10.00*** | 10.17*** |
| Model 2: AR(7)-L-X | 3.98*** | 4.41*** | 4.53*** | 4.68*** | 4.84*** | **4.96**** | **4.99**** | **5.44**** | **5.69**** | **5.82**** | **5.87**** | 6.01*** | **6.17**** | 6.31*** |
| Model 3: AR(7)-L-X-H | 3.86*** | 4.42*** | 4.67*** | 4.93*** | 5.21*** | 5.45*** | 5.59*** | 6.78*** | 8.20*** | 9.05*** | 8.74*** | 8.43*** | 8.20*** | 8.05*** |
| Model 4: AR(7)-L-X-S | 3.94*** | 4.37*** | **4.50**** | **4.66**** | **4.83**** | 4.96*** | 5.02*** | 5.57*** | 5.92*** | 6.07*** | 6.12*** | 6.24*** | 6.40*** | 6.53*** |
| Model 5: AR(7)-L-X-W | 3.98*** | 4.41*** | 4.53*** | 4.69*** | 4.85*** | **4.96**** | 5.00*** | 5.46*** | 5.71*** | 5.85*** | **5.87**** | **6.00**** | **6.17**** | **6.30**** |
| Model 6: AR(7)-L-Seas/trend | 4.12*** | 4.70*** | 4.95*** | 5.30*** | 5.56*** | 5.86*** | 6.04*** | 7.66*** | 10.38 | 13.11 | 14.75 | 15.93 | 16.83 | 17.63 |
| Model 7: AR(7)-L-X-Seas/trend | 4.01*** | 4.43*** | 4.58*** | 4.74*** | 4.92*** | 5.05*** | 5.09*** | 5.61*** | 6.20*** | 6.91*** | 7.21*** | 7.39*** | 7.24*** | 7.34*** |
| Model 8: AR(7)-L-X-H-Seas/trend | **3.82**** | **4.35**** | 4.61*** | 4.86*** | 5.12*** | 5.38*** | 5.51*** | 6.68*** | 8.58*** | 10.32 | 10.64 | 10.56 | 10.00*** | 9.75*** |
| Model 9: AR(7)-L-X-S-Seas/trend | 3.98*** | 4.40*** | 4.55*** | 4.73*** | 4.92*** | 5.07*** | 5.13*** | 5.76*** | 6.51*** | 7.26*** | 7.52*** | 7.64*** | 7.48*** | 7.60*** |
| Model 10: AR(7)-L-X-W-Seas/trend | 4.01*** | 4.43*** | 4.58*** | 4.75*** | 4.93*** | 5.06*** | 5.11*** | 5.63*** | 6.24*** | 6.96*** | 7.22*** | 7.39*** | 7.26*** | 7.35*** |
| **FFNN** | **1D** | **2D** | **3D** | **4D** | **5D** | **6D** | **7D** | **14D** | **1M** | **2M** | **3M** | **4M** | **5M** | **6M** |
| **Panel A: No Input Variables** | | | | | | | | | | | | | | |
| Naïve | 6.32 | 8.65 | 9.35 | 9.69 | 9.38 | 8.35 | 7.51 | 9.21 | 11.66 | **11.98** | **12.37** | **14.30** | **16.63** | **17.30** |
| FFNNAR(7, 10, 5) | **5.49** | **6.55** | **6.90** | **7.10** | **7.03** | **6.97** | **7.29** | **9.02** | **11.58** | 16.78 | 23.57 | 27.23 | 32.06 | 33.51 |
| **Panel B: With Actual Input Variables** | | | | | | | | | | | | | | |
| Model 1: FFNNAR(7, 10, 5)-L | 5.31 | 6.39 | 7.01 | 7.63 | 8.03 | 8.45 | 9.36 | 13.31 | 15.97 | 18.58 | 17.67*** | 17.11*** | 17.10*** | 18.14*** |
| Model 2: FFNNAR(7, 10, 5)-L-X | 4.75*** | 5.30*** | 5.87*** | 6.14*** | 6.39*** | 6.63*** | 7.10*** | 8.12*** | 9.75*** | 10.74*** | 10.37*** | 10.60*** | 10.28*** | 11.48*** |
| Model 3: FFNNAR(7, 10, 5)-L-X-H | 4.79 | 5.41 | 5.86 | 6.15** | 6.19 | 6.36 | 6.72 | 9.13 | 12.41 | 13.15*** | 12.87*** | 13.60*** | 13.47*** | 13.64*** |
| Model 4: FFNNAR(7, 10, 5)-L-X-S | 4.73*** | 5.38*** | 6.06** | 5.99** | 5.93** | 6.40** | 7.01 | 8.28 | 9.71** | 10.11*** | 9.67*** | 9.44*** | 9.48*** | 11.52*** |
| Model 5: FFNNAR(7, 10, 5)-L-X-W | 4.76*** | 5.41*** | 6.04*** | 6.16*** | 6.09*** | 6.36*** | 6.92*** | 8.45 | 10.08*** | 10.76*** | 10.29*** | 10.24*** | 10.27*** | 11.14*** |
| Model 6: FFNNAR(7, 10, 5)-L-Seas/trend | 5.24 | 6.11 | 6.67 | 7.24 | 7.53 | 7.93 | 8.22 | 10.06 | 12.21 | 13.86*** | 14.57*** | 14.27*** | 14.33*** | 14.11*** |
| Model 7: FFNNAR(7, 10, 5)-L-X-Seas/trend | **4.72**** | 5.22*** | 5.50*** | 5.68*** | 5.76*** | 5.59** | **5.60**** | **6.12**** | **6.88**** | **6.99**** | **6.68**** | 6.79*** | 7.50*** | 8.14*** |

(*continued on next page*)

**Table 2** (*continued*)

| Time Series | 1D | 2D | 3D | 4D | 5D | 6D | 7D | 14D | 1M | 2M | 3M | 4M | 5M | 6M |
|---|---|---|---|---|---|---|---|---|---|---|---|---|---|---|
| Model 8: FFNNAR(7, 10, 5)-L-X-H-Seas/trend | 4.76*** | 5.24*** | **5.40*** | **5.55*** | **5.66*** | 5.68*** | 5.85*** | 6.48*** | **6.88*** | 7.91*** | 8.56*** | 9.72*** | 10.26*** | 11.32*** |
| Model 9: FFNNAR(7, 10, 5)-L-X-S-Seas/trend | 4.73*** | 5.27*** | 5.71*** | 5.67*** | 5.95** | 5.99* | 6.03** | 6.42*** | 7.02*** | 7.01*** | 6.74*** | **6.28*** | **7.13*** | **7.70*** |
| Model10:FFNNAR(7, 10, 5)-L-X-W-Seas/trend | **4.72**** | **5.17*** | 5.47*** | 5.69*** | 5.72*** | **5.50*** | 5.70*** | 6.26*** | 7.02*** | 7.11*** | 6.77*** | 7.03*** | 7.36*** | 8.23*** |

Notes: Bolded cells indicate forecasts with the highest accuracy for each horizon within individual panels, while grey-shaded cells highlight the most accurate forecasts for each horizon across the entire table. The variable L denotes load; X includes the weighted import price and natural gas price; and H, S, and W represent hydroelectric, solar PV, and onshore wind generation, respectively. The term *"Seas/trend"* refers to models incorporating Fourier terms, monthly dummy variables, and a linear time trend. Asterisks (***, **, *) indicate statistical significance at the 1 %, 5 %, and 10 % levels, respectively, based on the Diebold-Mariano test. In the *Time Series* section, the Diebold-Mariano test compares the RMSEs in Panel B to those from the *AR(7)* benchmark in Panel A. In the *FFNN* section, the test compares RMSEs in Panel B to those from the *FFNNAR*(7, 10, 5) benchmark in Panel A.

**Table 3**
RMSE for ex-post forecasts of electricity prices in 2024.

| TimeSeries | 1D | 2D | 3D | 4D | 5D | 6D | 7D | 14D | 1M | 2M | 3M | 4M | 5M | 6M |
|---|---|---|---|---|---|---|---|---|---|---|---|---|---|---|
| **Panel A: No Input Variables** | | | | | | | | | | | | | | |
| Naive | 11.94 | 15.09 | 16.67 | 17.34 | 16.68 | 15.59 | 14.52 | **15.47** | **19.80** | **25.43** | **27.21** | **30.32** | **33.91** | **34.16** |
| Holt-Winters | **9.62** | **11.40** | **12.29** | **13.10** | **13.56** | **13.95** | 14.50 | 16.63 | 21.08 | 30.93 | 41.16 | 52.72 | 61.98 | 65.11 |
| AR(7) | 11.16 | 12.89 | 13.79 | 14.24 | 14.09 | 14.22 | **14.43** | 16.53 | 24.88 | 40.66 | 55.25 | 67.04 | 76.32 | 83.23 |
| **Panel B: With Actual Input Variables** | | | | | | | | | | | | | | |
| Model 1: AR(7)-L | 12.87 | 15.66 | 16.20 | 16.76 | 16.81 | 16.61 | 17.10 | 21.81 | 31.54 | 47.57 | 61.70 | 73.64 | 82.84 | 89.35 |
| Model 2: AR(7)-L-X | 10.22 | 11.39** | 11.64*** | 12.26** | 12.45** | 12.68** | 12.98** | 14.11*** | 15.06*** | 15.60*** | 15.88*** | 16.10*** | 16.18*** | 16.21*** |
| Model 3: AR(7)-L-X-H | 10.22 | **11.32**** | **11.51***** | **12.07***** | **12.20**** | **12.36**** | **12.58**** | **13.30***** | **13.52***** | **13.94***** | **14.29***** | **14.70***** | **14.90***** | **15.04***** |
| Model 4: AR(7)-L-X-S | **10.11** | 11.36** | 11.75*** | 12.45** | 12.69** | 12.96* | 13.30* | 14.70** | 16.04*** | 16.83*** | 17.01*** | 17.12*** | 17.13*** | 17.03*** |
| Model 5: AR(7)-L-X-W | 10.24 | 11.43** | 11.69*** | 12.32** | 12.52** | 12.76** | 13.07* | 14.21*** | 15.13*** | 15.61*** | 15.87*** | 16.16*** | 16.21*** | 16.18*** |
| Model 6: AR(7)-L-Seas/trend | 12.99 | 15.69 | 15.70 | 16.26 | 16.55 | 16.33 | 16.51 | 21.42 | 32.91 | 51.32 | 66.02 | 78.15 | 83.29 | 84.09 |
| Model 7: AR(7)-L-X-Seas/trend | 10.51 | 11.71 | 11.79** | 12.42** | 12.52** | 12.73** | 12.98* | 14.67** | 16.00*** | 16.89*** | 17.74*** | 17.82*** | 18.14*** | 18.66*** |
| Model 8: AR(7)-L-X-H-Seas/trend | 10.55 | 11.77 | 11.81** | 12.41** | 12.50** | 12.66** | 12.85* | 14.42** | 15.88*** | 17.12*** | 18.26*** | 18.13*** | 18.49*** | 18.78*** |
| Model 9: AR(7)-L-X-S-Seas/trend | 10.35 | 11.65* | 11.89*** | 12.58** | 12.75** | 12.97*** | 13.24*** | 15.26 | 17.14*** | 18.53*** | 19.50*** | 19.52*** | 19.59*** | 19.81*** |
| Model 10: AR(7)-L-X-W-Seas/trend | 10.53 | 11.74 | 11.83** | 12.46** | 12.57** | 12.78* | 13.05* | 14.74* | 16.09*** | 16.88*** | 17.77*** | 17.95*** | 18.23*** | 18.74*** |
| **FFNN** | **1D** | **2D** | **3D** | **4D** | **5D** | **6D** | **7D** | **14D** | **1M** | **2M** | **3M** | **4M** | **5M** | **6M** |
| **Panel A: No Input Variables** | | | | | | | | | | | | | | |
| Naïve | 11.94 | 15.09 | 16.67 | 17.34 | 16.68 | 15.59 | 14.52 | 15.47 | 19.80 | 25.43 | 27.21 | 30.32 | 33.91 | 34.16 |
| FFNNAR(7, 10, 5) | **10.43** | **12.31** | **13.16** | **13.53** | **13.98** | **13.90** | **14.00** | **15.36** | **19.19** | **22.03** | **23.69** | **26.01** | **26.20** | **25.34** |
| **Panel B: With Actual Input Variables** | | | | | | | | | | | | | | |
| Model 1: FFNNAR(7, 10, 5)-L | 10.34 | 12.18 | 13.32 | 14.31 | 15.21 | 15.93 | 16.77 | 20.08 | 19.21 | 21.34 | 22.26 | 21.85 | 23.55 | 27.20 |
| Model 2: FFNNAR(7, 10, 5)-L-X | 8.94* | 10.14*** | 10.68*** | 11.02*** | 11.52*** | 11.66*** | 12.08*** | 13.05*** | 13.48*** | 14.76*** | 15.81*** | 14.74*** | **13.79***** | 17.90*** |
| Model 3: FFNNAR(7, 10, 5)-L-X-H | 8.86** | **9.74***** | **10.30***** | **10.54***** | **10.75***** | **10.88***** | **11.29**** | **12.53** | 14.36 | 18.17 | 20.13 | 19.87 | 18.86 | 18.71 |
| Model 4: FFNNAR(7, 10, 5)-L-X-S | **8.69** | 9.76*** | 10.40*** | 10.89*** | 11.41** | 11.70** | 11.96* | 12.90*** | **12.44***** | 15.32*** | 17.81*** | 18.31*** | 16.81** | 17.31** |
| Model 5: FFNNAR(7, 10, 5)-L-X-W | 9.09* | 10.21** | 10.88*** | 11.32*** | 11.82** | 11.96** | 12.26** | 13.09** | 12.76*** | **14.09***** | **15.10***** | **14.64***** | 14.24*** | **16.10***** |
| Model 6: FFNNAR(7, 10, 5)-L-Seas/trend | 11.13 | 13.39 | 15.35 | 16.70 | 18.26 | 19.94 | 21.81 | 31.34 | 48.48 | 57.47 | 49.93 | 50.88 | 68.86 | 52.90 |
| Model 7: FFNNAR(7, 10, 5)-L-X-Seas/trend | 10.29 | 11.45* | 12.26 | 13.31 | 14.09 | 14.48 | 15.22 | 17.41 | 20.60 | 20.50 | 21.35* | 21.43*** | 23.09*** | 24.35 |
| Model 8: FFNNAR(7, 10, 5)-L-X-H-Seas/trend | 10.02 | 11.44 | 12.23** | 12.92 | 13.69 | 14.07 | 14.91 | 17.62 | 23.59 | 24.43 | 25.66 | 27.58 | 30.06 | 32.99 |

(*continued on next page*)

**Table 3** (*continued*)

| Time Series | 1D | 2D | 3D | 4D | 5D | 6D | 7D | 14D | 1M | 2M | 3M | 4M | 5M | 6M |
|---|---|---|---|---|---|---|---|---|---|---|---|---|---|---|
| Model 9: FFNNAR(7, 10, 5)-L-X-S-Seas/trend | 10.13 | 11.35 | 12.56 | 13.65 | 14.64 | 15.28 | 15.59 | 18.16 | 21.57 | 22.66 | 22.38 | 22.60*** | 23.38** | 25.97 |
| Model10: FFNNAR(7, 10, 5)-L-X-W-Seas/trend | 10.22 | 11.78 | 12.75 | 13.24 | 14.03 | 14.72 | 14.94 | 17.56 | 22.30 | 21.67 | 23.16 | 23.05** | 23.66** | 28.43 |

Notes: Bolded cells indicate forecasts with the highest accuracy for each horizon within individual panels, while grey-shaded cells highlight the most accurate forecasts for each horizon across the entire table. The variable L denotes load; X includes the weighted import price and natural gas price; and H, S, and W represent hydroelectric, solar PV, and onshore wind generation, respectively. The term *"Seas/trend"* refers to models incorporating Fourier terms, monthly dummy variables, and a linear time trend. Asterisks (***, **, *) indicate statistical significance at the 1 %, 5 %, and 10 % levels, respectively, based on the Diebold-Mariano test. In the *Time Series* section, the Diebold-Mariano test compares the RMSEs in Panel B to those from the *AR*(7) benchmark in Panel A. In the *FFNN* section, the test compares RMSEs in Panel B to those from the *FFNNAR*(7, 10, 5) benchmark in Panel A.

**Table 4**
MAPE for ex-post forecasts of electricity prices in 2019.

| Time Series | 1D | 2D | 3D | 4D | 5D | 6D | 7D | 14D | 1M | 2M | 3M | 4M | 5M | 6M |
|---|---|---|---|---|---|---|---|---|---|---|---|---|---|---|
| **Panel A: No Input Variables** | | | | | | | | | | | | | | |
| Naive | 10.00 | 14.27 | 15.43 | 16.10 | 15.88 | 13.67 | 11.92 | 15.00 | 19.83 | 20.54 | 21.35 | 25.09 | 28.77 | 30.54 |
| Holt-Winters | **7.69** | **8.95** | **9.68** | **10.40** | **11.08** | **11.24** | **11.66** | **14.45** | **16.49** | **17.67** | 22.89 | 28.29 | 32.49 | 37.59 |
| AR(7) | 8.89 | 10.89 | 11.38 | 11.75 | 12.02 | 12.07 | 12.40 | 15.77 | 17.68 | 19.23 | **19.89** | **20.83** | **21.56** | **21.53** |
| **Panel B: With Actual Input Variables** | | | | | | | | | | | | | | |
| Model 1: AR(7)-L | 6.40 | 7.24 | 7.63 | 8.17 | 8.60 | 8.94 | 9.17 | 11.12 | 14.23 | 16.55 | 17.09 | 17.84 | 18.15 | 18.24 |
| Model 2: AR(7)-L-X | 6.23 | 6.98 | 7.14 | 7.42 | **7.74** | 7.97 | 8.02 | 9.06 | **9.49** | **9.61** | **9.58** | **9.69** | **9.93** | **10.11** |
| Model 3: AR(7)-L-X-H | 6.06 | 7.09 | 7.59 | 8.04 | 8.55 | 8.97 | 9.25 | 11.51 | 14.34 | 16.37 | 15.89 | 15.41 | 14.90 | 14.32 |
| Model 4: AR(7)-L-X-S | 6.22 | 6.96 | 7.14 | 7.44 | 7.78 | 8.04 | 8.14 | 9.31 | 9.93 | 10.07 | 10.06 | 10.14 | 10.36 | 10.58 |
| Model 5: AR(7)-L-X-W | 6.22 | 6.98 | **7.13** | **7.41** | **7.74** | **7.96** | **8.01** | **9.05** | 9.51 | 9.66 | 9.60 | 9.69 | 9.93 | 10.09 |
| Model 6: AR(7)-L-Seas/trend | 6.57 | 7.68 | 8.22 | 8.97 | 9.59 | 10.09 | 10.55 | 13.38 | 18.66 | 23.97 | 26.80 | 29.28 | 31.72 | 33.59 |
| Model 7: AR(7)-L-X-Seas/trend | 6.42 | 7.20 | 7.53 | 7.87 | 8.28 | 8.55 | 8.63 | 9.64 | 10.86 | 12.25 | 12.70 | 13.02 | 12.59 | 12.54 |
| Model 8: AR(7)-L-X-H-Seas/trend | **6.03** | **6.95** | 7.43 | 7.94 | 8.39 | 8.79 | 9.07 | 11.09 | 14.73 | 18.31 | 19.02 | 18.79 | 17.30 | 16.55 |
| Model 9: AR(7)-L-X-S-Seas/trend | 6.37 | 7.14 | 7.47 | 7.86 | 8.30 | 8.55 | 8.70 | 9.92 | 11.39 | 12.89 | 13.30 | 13.50 | 13.04 | 12.96 |
| Model 10: AR(7)-L-X-W-Seas/trend | 6.42 | 7.20 | 7.52 | 7.86 | 8.27 | 8.54 | 8.63 | 9.67 | 10.92 | 12.33 | 12.70 | 13.01 | 12.59 | 12.55 |
| **FFNN** | **1D** | **2D** | **3D** | **4D** | **5D** | **6D** | **7D** | **14D** | **1M** | **2M** | **3M** | **4M** | **5M** | **6M** |
| **Panel A: No Input Variables** | | | | | | | | | | | | | | |
| Naive | 10.00 | 14.27 | 15.43 | 16.10 | 15.88 | 13.67 | 11.92 | **15.00** | **19.83** | **20.54** | **21.35** | **25.09** | **28.77** | **30.54** |
| FFNNAR(7, 10, 5) | **9.08** | **10.55** | **11.22** | **11.57** | **11.46** | **11.32** | **11.78** | 15.31 | 20.86 | 30.62 | 43.20 | 49.89 | 59.78 | 62.55 |
| **Panel B: With Actual Input Variables** | | | | | | | | | | | | | | |
| Model 1: FFNNAR(7, 10, 5)-L | 8.46 | 10.38 | 11.16 | 11.80 | 12.41 | 13.57 | 15.10 | 20.48 | 25.53 | 27.58 | 26.16 | 24.84 | 24.59 | 24.99 |
| Model 2: FFNNAR(7, 10, 5)-L-X | 7.23 | 8.14 | 8.65 | 9.05 | 8.94 | 9.24 | 9.97 | 11.69 | 14.01 | 15.02 | 13.64 | 13.78 | 14.57 | 15.37 |
| Model 3: FFNNAR(7, 10, 5)-L-X-H | 8.10 | 9.22 | 9.51 | 9.62 | 9.82 | 10.07 | 10.75 | 13.49 | 17.49 | 18.77 | 16.83 | 17.77 | 18.93 | 20.09 |
| Model 4: FFNNAR(7, 10, 5)-L-X-S | 7.23 | 8.28 | 8.92 | 9.23 | 9.46 | 9.55 | 10.68 | 12.92 | 14.91 | 14.50 | 12.64 | 13.78 | 14.77 | 17.29 |
| Model 5: FFNNAR(7, 10, 5)-L-X-W | **7.22** | 8.19 | 8.79 | 9.08 | 9.35 | 9.53 | 10.04 | 11.37 | 13.78 | 14.55 | 12.99 | 13.81 | 14.41 | 15.51 |
| Model 6: FFNNAR(7, 10, 5)-L-Seas/trend | 8.02 | 9.66 | 10.59 | 11.71 | 12.08 | 12.79 | 13.29 | 17.61 | 23.72 | 26.55 | 26.74 | 25.56 | 23.55 | 25.55 |
| Model 7: FFNNAR(7, 10, 5)-L-X-Seas/trend | 7.25 | **7.90** | 8.27 | 8.46 | **8.44** | 8.68 | 9.03 | 10.01 | 12.05 | 12.56 | 11.88 | 11.69 | **12.28** | 13.89 |
| Model 8: FFNNAR(7, 10, 5)-L-X-H-Seas/trend | 7.47 | 8.15 | 8.69 | 8.75 | 8.72 | 8.89 | 9.03 | 10.28 | 12.58 | 13.63 | 14.44 | 16.33 | 16.98 | 19.10 |
| Model 9: FFNNAR(7, 10, 5)-L-X-S-Seas/trend | 7.30 | 7.92 | **8.10** | **8.38** | 9.07 | 8.79 | 8.70 | 9.98 | **11.55** | **11.72** | **11.37** | **11.30** | 12.39 | 13.38 |
| Model10: FFNNAR(7, 10, 5)-L-X-W-Seas/trend | 7.51 | 8.08 | 8.23 | 8.65 | 8.80 | **8.48** | **8.69** | **9.82** | 11.78 | 12.16 | 11.63 | 12.27 | 12.85 | **12.98** |

Notes: Bolded cells indicate forecasts with the highest accuracy for each horizon within individual panels, while grey-shaded cells highlight the most accurate forecasts for each horizon across the entire table. The variable L denotes load; X includes the weighted import price and natural gas price; and H, S, and W represent hydroelectric, solar PV, and onshore wind generation, respectively. The term *"Seas/trend"* refers to models incorporating Fourier terms, monthly dummy variables, and a linear time trend.

**Table 5**
MAPE for ex-post forecasts of electricity prices in 2024.

| Time Series | 1D | 2D | 3D | 4D | 5D | 6D | 7D | 14D | 1M | 2M | 3M | 4M | 5M | 6M |
|---|---|---|---|---|---|---|---|---|---|---|---|---|---|---|
| **Panel A: No Input Variables** | | | | | | | | | | | | | | |
| Naive | 8.41 | 11.01 | 12.32 | 12.93 | 12.39 | 11.44 | 10.39 | **11.06** | **15.01** | **19.14** | **21.68** | **24.33** | **26.99** | **27.35** |
| Holt-Winters | **6.96** | **8.16** | **8.80** | **9.29** | **9.34** | **9.82** | **10.33** | 11.76 | 15.14 | 23.32 | 32.31 | 39.38 | 45.73 | 49.43 |
| AR(7) | 8.13 | 9.44 | 10.24 | 10.69 | 10.51 | 10.54 | 10.70 | 13.13 | 20.55 | 33.94 | 47.35 | 59.34 | 69.97 | 78.01 |
| **Panel B: With Actual Input Variables** | | | | | | | | | | | | | | |
| Model 1: AR(7)-L | 8.97 | 11.58 | 11.95 | 12.37 | 12.28 | 11.95 | 12.45 | 15.80 | 23.86 | 37.50 | 52.21 | 65.27 | 74.74 | 82.45 |
| Model 2: AR(7)-L-X | 7.11 | 8.20 | 8.40 | 8.77 | 9.02 | 9.08 | 9.38 | 10.18 | 11.14 | 11.57 | 11.83 | 12.04 | 12.04 | 11.96 |
| Model 3: AR(7)-L-X-H | **7.06** | **8.11** | **8.23** | **8.56** | **8.75** | **8.77** | **9.00** | **9.43** | **10.04** | **10.44** | **10.74** | **11.08** | **11.21** | **11.28** |
| Model 4: AR(7)-L-X-S | 7.08 | 8.16 | 8.49 | 8.92 | 9.25 | 9.27 | 9.61 | 10.64 | 11.96 | 12.50 | 12.69 | 12.82 | 12.76 | 12.61 |
| Model 5: AR(7)-L-X-W | 7.12 | 8.23 | 8.44 | 8.81 | 9.08 | 9.14 | 9.43 | 10.25 | 11.19 | 11.60 | 11.81 | 12.05 | 12.03 | 11.88 |
| Model 6: AR(7)-L-Seas/trend | 9.23 | 11.38 | 11.43 | 11.71 | 11.89 | 11.60 | 11.33 | 15.41 | 24.89 | 39.17 | 48.41 | 55.23 | 60.35 | 64.26 |
| Model 7: AR(7)-L-X-Seas/trend | 7.22 | 8.33 | 8.41 | 8.83 | 8.97 | 9.10 | 9.25 | 10.10 | 11.07 | 12.12 | 12.35 | 12.68 | 12.88 | 13.19 |
| Model 8: AR(7)-L-X-H-Seas/trend | 7.22 | 8.33 | 8.37 | 8.74 | 8.88 | 8.97 | 9.12 | 9.75 | 10.88 | 12.28 | 12.82 | 12.93 | 13.10 | 13.46 |
| Model 9: AR(7)-L-X-S-Seas/trend | 7.20 | 8.36 | 8.56 | 9.03 | 9.22 | 9.33 | 9.49 | 10.70 | 12.21 | 13.58 | 13.89 | 14.07 | 14.02 | 14.12 |
| Model 10: AR(7)-L-X-W-Seas/trend | 7.23 | 8.35 | 8.43 | 8.86 | 9.02 | 9.14 | 9.29 | 10.15 | 11.13 | 12.11 | 12.37 | 12.73 | 12.93 | 13.26 |
| **FFNN** | **1D** | **2D** | **3D** | **4D** | **5D** | **6D** | **7D** | **14D** | **1M** | **2M** | **3M** | **4M** | **5M** | **6M** |
| **Panel A: No Input Variables** | | | | | | | | | | | | | | |
| Naive | 8.41 | 11.01 | 12.32 | 12.93 | 12.39 | 11.44 | 10.39 | **11.06** | 15.01 | 19.14 | 21.68 | 24.33 | 26.99 | 27.35 |
| FFNNAR(7, 10, 5) | **7.85** | **9.17** | **9.88** | **10.12** | **10.35** | **10.26** | **10.35** | 11.77 | **14.44** | **16.68** | **18.28** | **19.20** | **18.91** | **17.95** |
| **Panel B: With Actual Input Variables** | | | | | | | | | | | | | | |
| Model 1: FFNNAR(7, 10, 5)-L | 8.31 | 10.03 | 10.86 | 11.78 | 12.87 | 13.69 | 14.67 | 18.47 | 19.85 | 22.84 | 25.05 | 28.00 | 30.57 | 33.09 |
| Model 2: FFNNAR(7, 10, 5)-L-X | **6.95** | **7.77** | 8.21 | 8.55 | **8.71** | **8.70** | **8.82** | **9.66** | **10.31** | **12.31** | **12.70** | **12.53** | **11.53** | **11.33** |
| Model 3: FFNNAR(7, 10, 5)-L-X-H | 6.85 | 7.80 | **8.02** | **8.49** | 8.99 | 8.95 | 9.22 | 10.37 | 13.00 | 16.77 | 16.20 | 17.53 | 18.46 | 15.45 |
| Model 4: FFNNAR(7, 10, 5)-L-X-S | 7.05 | 7.82 | 8.27 | 8.60 | 9.05 | 9.03 | 9.33 | 9.99 | 10.69 | 13.78 | 15.01 | 15.38 | 15.67 | 14.94 |
| Model 5: FFNNAR(7, 10, 5)-L-X-W | 7.11 | 8.08 | 8.29 | 8.67 | 9.15 | 9.10 | 9.16 | 10.10 | 10.44 | 12.71 | 13.08 | 12.87 | 12.51 | 11.90 |
| Model 6: FFNNAR(7, 10, 5)-L-Seas/trend | 8.44 | 9.87 | 11.57 | 12.22 | 13.51 | 14.88 | 15.56 | 20.22 | 27.63 | 38.44 | 38.33 | 44.12 | 45.28 | 34.98 |
| Model 7: FFNNAR(7, 10, 5)-L-X-Seas/trend | 7.79 | 8.98 | 9.39 | 10.06 | 10.44 | 10.76 | 11.01 | 13.00 | 16.24 | 16.91 | 16.65 | 15.26 | 15.59 | 15.87 |
| Model 8: FFNNAR(7, 10, 5)-L-X-H-Seas/trend | 7.99 | 8.92 | 9.52 | 10.44 | 10.77 | 10.99 | 11.70 | 14.16 | 16.89 | 19.79 | 18.85 | 19.13 | 20.40 | 23.63 |
| Model 9: FFNNAR(7, 10, 5)-L-X-S-Seas/trend | 7.77 | 8.70 | 9.14 | 9.85 | 10.04 | 10.67 | 11.23 | 12.35 | 16.09 | 17.31 | 16.30 | 16.38 | 17.37 | 19.95 |
| Model10:FFNNAR(7, 10, 5)-L-X-W-Seas/trend | 7.99 | 8.98 | 9.18 | 10.21 | 10.71 | 11.32 | 11.69 | 13.22 | 16.06 | 17.11 | 17.67 | 16.85 | 17.27 | 19.93 |

Notes: Bolded cells indicate forecasts with the highest accuracy for each horizon within individual panels, while grey-shaded cells highlight the most accurate forecasts for each horizon across the entire table. The variable L denotes load; X includes the weighted import price and natural gas price; and H, S, and W represent hydroelectric, solar PV, and onshore wind generation, respectively. The term *"Seas/trend"* refers to models incorporating Fourier terms, monthly dummy variables, and a linear time trend.

gains in forecast accuracy at short-term horizons (days 1–5), with RMSE decreases of less than 1 %. However, from day 6 onward, the RMSE values exceed those of Model 2, suggesting a limited and short-lived benefit from incorporating solar data. Model 5 shows no change in RMSE at short-term horizons and only minor improvements of less than 1 % at medium-term horizons. This suggests that the overall effect of solar and wind generation on price prediction is marginal.

Therefore, in 2019, the findings suggest a strong predictive power for load, weighted import prices, and natural gas prices across all forecast horizons. In contrast, wind and solar generation provide only modest predictive value, while hydropower generation consistently fails to enhance forecasting accuracy for electricity prices in Northern Italy. Therefore, the predictive contribution of RES variables remained limited in 2019.

The findings from the time series models are further confirmed by the results from the *FFNN* models reported in the second section of Table 2. While the general patterns of accuracy hold across both approaches, for the year 2019, the time series models tend to produce more accurate forecasts than the *FFNN* counterparts across all forecast horizons.

Fig. 10 visualizes the RMSE values as reported in Table 2, highlighting the outputs of Models 2 through 5 using both time series and *FFNN* approaches. In this figure, a consistent reduction in forecast accuracy is apparent as the forecast horizons extend.

In terms of forecasting accuracy, our best-performing model for the year 2019 achieves a RMSE of 3.82. This compares well with results from similar studies in the Italian electricity price forecasting literature. For instance, Gianfreda et al. (2020) reported a RMSE of 6.8 for day-ahead price forecasts in Italy during the 2016–2017 period. Billé et al. (2023) evaluated multiple forecasting models for the Northern Italian market, with one of their best-performing models generating a RMSE of about 5 for the year 2019. These comparisons suggest that our model provides a significant improvement in forecast accuracy relative to the existing benchmarks.

### 6.2.2. Year 2024

Turning to the year 2024, as presented in the time series section in of Table 3, the performance changes significantly compared to 2019. Forecast errors are consistently higher across all horizons, suggesting a general reduction in forecast accuracy. This decline can be attributed to several factors; two of the main reasons are outlined below.

First, the electricity market experienced substantial volatility between 2021 and 2023 (see Fig. 1), and this period forms the in-sample estimation window for the 2024 forecasts. These years experienced extreme price fluctuations, demand shocks, and supply disruptions, primarily linked to COVID-19 and geopolitical events, which introduced substantial noise into electricity price patterns. Furthermore, there was greater uncertainty in natural gas prices during this period. As a major driver of electricity costs, this volatility propagates through the forecasting models and reduces their accuracy.

Second, the generation mix became more complex by 2024 owing to a rise in the share of renewable energy sources, particularly solar and wind, across Europe. Their natural variability and weather dependence make electricity prices more difficult to predict, especially when using traditional time series approaches.

Focusing on the first section of Table 3, which represents time series accuracies, Model 1 that (adding load) performs worse than the *AR*(7) across almost all horizons in 2024 (e.g., the RMSE increases from 11.16 to 12.87 at one-day ahead and from 83.23 to 89.35 at six-months ahead), suggesting uncertainty due to higher market volatility. However, Model 2 (adding natural gas prices and weighted import prices) yields a significant performance improvement, cutting the RMSE at all horizons compared to Model 1 (e.g., from 31.54 to 15.06 at one-month ahead). The RMSE drops by an average of 20 %–80 % across horizons, with the most significant gains at medium

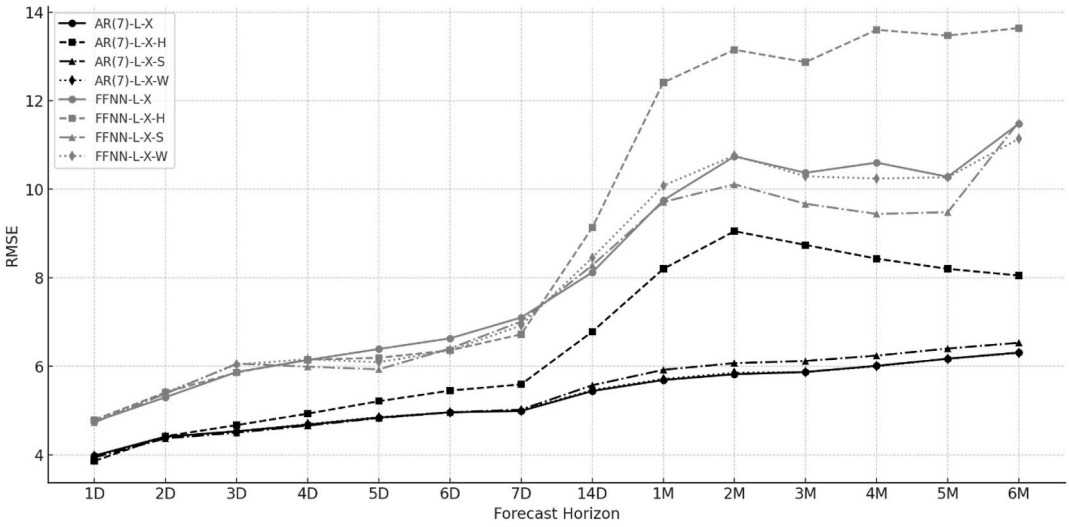



**Fig. 10.** RMSEs comparison for 2019.
Note: The variable L denotes load; X includes the weighted import price and natural gas price; and H, S, and W represent hydroelectric, solar PV, and onshore wind generation, respectively. The term *"Seas/trend"* refers to models incorporating Fourier terms, monthly dummy variables, and a linear time trend.

horizons. This underlines the increasing importance of cost drivers in recent electricity price formation.

Model 3 (adding hydro generation) consistently improves the RMSE over Model 2 across all horizons. The average RMSE improvement from Model 2 to Model 3 ranges from 0.6 % to 10 % across short- to medium- term horizons. This is an important contrast to 2019 and suggests that hydropower generation has become more predictive of electricity prices in 2024, possibly due to its larger market share. However, there is no evidence of a contribution from solar (Model 4) or wind (Model 5) generation, as their inclusion consistently increases the RMSE compared to Model 2.

From 2016 to 2024, the share of renewable energy sources in Northern Italy experienced notable changes. Hydropower held the highest share, rising from 20 % in 2016 to a peak of 29 % in 2024, indicating its dominant role in the region's electricity system. Solar generation also expanded steadily, increasing from 4 % in 2016 to 6.2 % in 2024. Wind power, while starting from a negligible base of 0.04 % in 2016, showed a modest increase, reaching 0.32 % by 2024. These trends suggest a shift in the energy mix, especially between 2019 and 2024, during which the predictive power of renewable variables in electricity price forecasting models became more apparent. Despite the increase in the predictive relevance of hydro generation, the overall forecast accuracy in 2024 was lower than in 2019. This paradox reflects the increasing difficulty and volatility of electricity markets as renewable energy becomes more deeply integrated into the system. Renewable generation introduces greater uncertainty into electricity price formation because of its dependence on weather conditions and the limited storability of electricity. While this growing volatility makes accurate forecasting more difficult, as is evident by the lower forecast accuracy for 2024 compared with 2019, it also enhances the value of renewable-aware forecasting models, as models that omit these variables are likely to become increasingly misaligned with market conditions.

A comparison between the forecasting accuracy of time series models and *FFNN*s reveals a notable shift from 2019 to 2024. In 2024, the *FFNN* models outperform their time series counterparts. For example, at the one-day ahead horizon, the best-performing time series model, *AR*(7)-*L*-*X*-*S*, yields an RMSE of 10.11, whereas the *FFNN* model with the same input structure, *FFNNAR*(7,10,5)-*L*-*X*-*S*, achieves a lower RMSE of 8.69. Across the two-day to two-weeks horizons, the *FFNNAR* (7,10,5)-*L*-*X*-*H* model, which includes hydropower generation, consistently produces the most accurate forecasts, outperforming all other models. The reason for this improvement is the *FFNN*'s ability to model complex and nonlinear relationships between electricity prices and input variables, such as natural gas prices and renewable generation sources, which have become increasingly important in recent years. This shows that data-driven machine learning approaches can outperform traditional statistical techniques in high-volatility environments.

Fig. 11 visualizes the RMSE values as reported in Table 3, highlighting the outputs of Models 2 through 5 using both time series and *FFNN* approaches.

Incorporating seasonality and trend components (Models 6–10) generally worsens the RMSE in both the 2019 and 2024 forecasts, suggesting potential overfitting or the inclusion of irrelevant features. This outcome is likely because the input variables already capture the underlying seasonal patterns in electricity prices, making additional seasonal terms redundant.

The MAPE values reported in Tables 4 and 5 for the years 2019 and 2024, respectively, are consistent with the conclusions drawn from the RMSE analysis.

### 6.2.3. *Further analysis*

Up until now, the focus has been on the forecasts generated by models utilizing the actual data of the input variables. These forecasts evaluate our models and determine the significance of the input variables. However, they are not genuine ex-ante forecasts, in

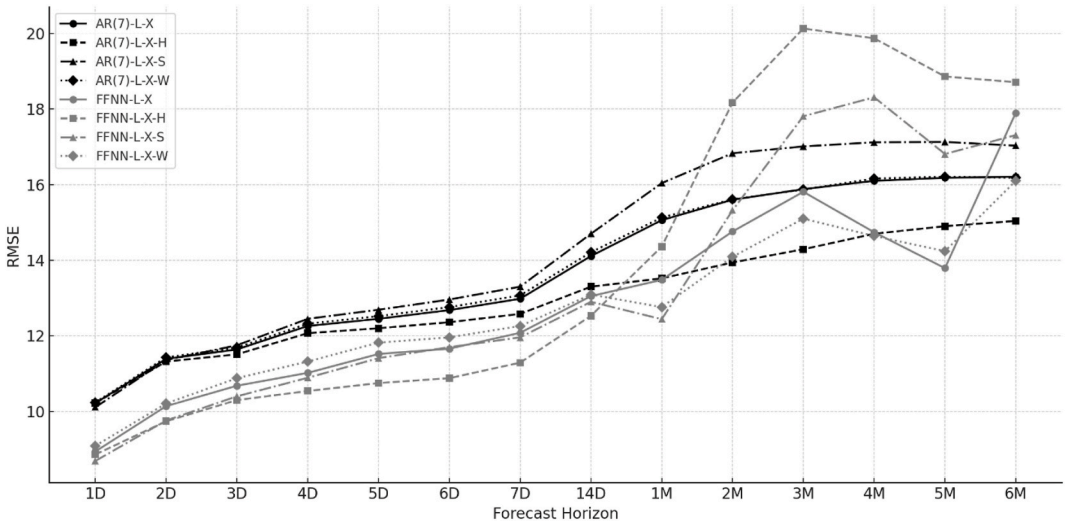



**Fig. 11.** RMSEs comparison for 2024.
Note: The variable L denotes load; X includes the weighted import price and natural gas price; and H, S, and W represent hydroelectric, solar PV, and onshore wind generation, respectively. The term *"Seas/trend"* refers to models incorporating Fourier terms, monthly dummy variables, and a linear time trend.

**Table 6**
RMSE for ex-ante forecasts of electricity prices in 2019.

| TimeSeries | 1D | 2D | 3D | 4D | 5D | 6D | 7D | 14D | 1M | 2M | 3M | 4M | 5M | 6M |
|---|---|---|---|---|---|---|---|---|---|---|---|---|---|---|
| **Panel A: No Input Variables** | | | | | | | | | | | | | | |
| Naive | 6.32 | 8.65 | 9.35 | 9.69 | 9.38 | 8.35 | 7.51 | 9.21 | 11.66 | 11.98 | 12.37 | 14.30 | 16.63 | 17.30 |
| Holt-Winters | **4.77** | **5.70** | **6.06** | **6.53** | **6.74** | **7.01** | **7.23** | **8.81** | **9.71** | 10.80 | 13.73 | 17.22 | 19.96 | 22.66 |
| AR(7) | 5.38 | 6.58 | 6.89 | 7.12 | 7.22 | 7.25 | 7.40 | 8.96 | 9.87 | **10.43** | **10.81** | **11.33** | **11.83** | **11.84** |
| **Panel B: With Actual Input Variables** | | | | | | | | | | | | | | |
| Model 1: AR(7)-L | **4.28***** | **5.02***** | **5.24***** | **5.51***** | **5.70***** | **5.90***** | **6.02***** | **7.05***** | 8.47*** | 9.43** | 9.64** | 10.08*** | 10.42*** | 10.55*** |
| Model 2: AR(7)-L-X | 4.46*** | 5.24*** | 5.52*** | 5.87*** | 6.10*** | 6.23*** | 6.43*** | 7.49*** | **8.14***** | **8.30***** | **8.43***** | **8.84***** | **9.84***** | **10.54***** |
| Model 3: AR(7)-L-X-H | 4.67*** | 5.63*** | 6.07*** | 6.64** | 7.07 | 7.42 | 7.79 | 9.93 | 12.08 | 13.02 | 13.46 | 13.99 | 14.67 | 15.39 |
| Model 4: AR(7)-L-X-S | 4.45*** | 5.25*** | 5.58*** | 5.99*** | 6.25*** | 6.42*** | 6.66*** | 7.88*** | 8.74*** | 9.27*** | 9.85*** | 10.43*** | 11.44* | 12.14 |
| Model 5: AR(7)-L-X-W | 4.46*** | 5.27*** | 5.60*** | 5.99*** | 6.25*** | 6.41*** | 6.64*** | 7.80*** | 8.63*** | 9.18*** | 9.80*** | 10.43*** | 11.44* | 12.13 |
| Model 6: AR(7)-L-Seas/trend | 4.40*** | 5.34*** | 5.77*** | 6.18*** | 6.50*** | 6.80** | 7.04** | 8.69 | 11.17 | 13.67 | 15.36 | 16.50 | 17.47 | 18.34 |
| Model 7: AR(7)-L-X-Seas/trend | 4.51*** | 5.39*** | 5.84*** | 6.30*** | 6.64*** | 6.89** | 7.19 | 8.75 | 10.23 | 11.20 | 11.89 | 12.38 | 12.97 | 13.54 |
| Model 8: AR(7)-L-X-H-Seas/trend | 4.63*** | 5.64*** | 6.17*** | 6.78* | 7.24 | 7.64 | 8.05 | 10.38 | 13.15 | 14.53 | 14.91 | 15.03 | 15.11 | 15.48 |
| Model 9: AR(7)-L-X-S-Seas/trend | 4.50*** | 5.37*** | 5.82*** | 6.29*** | 6.64*** | 6.89** | 7.21 | 8.83 | 10.38 | 11.35 | 12.00 | 12.42 | 13.00 | 13.60 |
| Model 10: AR(7)-L-X-W-Seas/trend | 4.51*** | 5.40*** | 5.84*** | 6.31*** | 6.65*** | 6.89** | 7.20 | 8.76 | 10.23 | 11.20 | 11.88 | 12.36 | 12.93 | 13.49 |
| **FFNN** | **1D** | **2D** | **3D** | **4D** | **5D** | **6D** | **7D** | **14D** | **1M** | **2M** | **3M** | **4M** | **5M** | **6M** |
| **Panel A: No Input Variables** | | | | | | | | | | | | | | |
| Naive | 6.32 | 8.65 | 9.35 | 9.69 | 9.38 | 8.35 | 7.51 | 9.21 | 11.66 | **11.98** | **12.37** | **14.30** | **16.63** | **17.30** |
| FFNNAR(7, 10, 5) | **5.49** | **6.55** | **6.90** | **7.10** | **7.03** | **6.97** | **7.29** | **9.02** | **11.58** | 16.78 | 23.57 | 27.23 | 32.06 | 33.51 |
| **Panel B: With Actual Input Variables** | | | | | | | | | | | | | | |
| Model 1: FFNNAR(7, 10, 5)-L | 5.08** | 6.16** | 6.53 | 6.92 | 7.17 | 7.53 | 8.03 | 10.28 | 13.66 | 16.30 | 16.84*** | 17.78*** | 18.64*** | 19.40*** |
| Model 2: FFNNAR(7, 10, 5)-L-X | 5.29 | 6.32 | 6.70 | 6.72* | 6.98 | 7.10 | 7.61 | 9.58 | 11.12 | 11.75*** | 12.04*** | 12.26*** | 12.75*** | 13.32*** |
| Model 3: FFNNAR(7, 10, 5)-L-X-H | 5.15 | 6.30 | 7.05 | 7.51 | 7.72 | 7.44 | 8.24 | 12.61 | 15.58 | 17.39 | 17.61*** | 16.75*** | 15.15*** | 14.11*** |
| Model 4: FFNNAR(7, 10, 5)-L-X-S | 5.19* | 6.03** | 6.61 | 7.01 | **7.01** | **7.04** | **7.40** | 9.08 | 11.34 | 11.74*** | 11.62*** | 11.93*** | 12.49*** | 13.79*** |
| Model 5: FFNNAR(7, 10, 5)-L-X-W | 5.23 | 6.06** | 6.59 | 6.80 | 6.94 | 7.22 | 7.73 | 9.38 | 11.26 | 11.47*** | 11.59*** | 11.94*** | 12.65*** | 13.40*** |
| Model 6: FFNNAR(7, 10, 5)-L-Seas/trend | 5.20* | 6.38 | 6.65 | 7.24 | 7.95 | 8.07 | 8.58 | 10.63 | 13.02 | 14.04*** | 14.45*** | 15.13*** | 15.32*** | 15.08*** |
| Model 7: FFNNAR(7, 10, 5)-L-X-Seas/trend | **5.00**** | 5.94** | **6.45*** | **6.82** | 7.21 | 7.51 | 7.53 | 9.08 | 10.85** | 11.43*** | 11.63*** | 12.09*** | 12.96*** | **13.09***** |

(*continued on next page*)

**Table 6** (*continued*)

| Time Series | 1D | 2D | 3D | 4D | 5D | 6D | 7D | 14D | 1M | 2M | 3M | 4M | 5M | 6M |
|---|---|---|---|---|---|---|---|---|---|---|---|---|---|---|
| Model 8: FFNNAR(7, 10, 5)-L-X-H-Seas/ trend | 5.13* | **5.91**** | 6.53* | 6.86 | 7.12 | 7.38 | 7.77 | 9.07 | **10.73**** | **10.85***** | **11.42***** | **11.70***** | **12.78***** | 13.37*** |
| Model 9: FFNNAR(7, 10, 5)-L-X-S-Seas/ trend | 5.12** | **5.91**** | 6.62 | 7.06 | 7.08 | 7.37 | 7.53 | **9.05** | 10.82** | 11.48*** | 11.87*** | 12.18*** | 12.86*** | 13.46*** |
| Model10:FFNNAR(7, 10, 5)-L-X-W-Seas/ trend | 5.14* | 5.97** | 6.44* | 7.01 | 7.24 | 7.38 | 7.90 | 9.40 | 10.75** | 11.31*** | 11.72*** | 11.90*** | **12.78***** | 13.26*** |

Notes: Bolded cells indicate forecasts with the highest accuracy for each horizon within individual panels, while grey-shaded cells highlight the most accurate forecasts for each horizon across the entire table. The variable L denotes load; X includes the weighted import price and natural gas price; and H, S, and W represent hydroelectric, solar PV, and onshore wind generation, respectively. The term *"Seas/trend"* refers to models incorporating Fourier terms, monthly dummy variables, and a linear time trend. Asterisks (***, **, *) indicate statistical significance at the 1 %, 5 %, and 10 % levels, respectively, based on the Diebold-Mariano test. In the *Time Series* section, the Diebold-Mariano test compares the RMSEs in Panel B to those from the AR (7) benchmark in Panel A. In the *FFNN* section, the test compares RMSEs in Panel B to those from the FFNNAR (7, 10, 5) benchmark in Panel A.

**Table 7**
RMSE for ex-ante forecasts of electricity prices in 2024.

| TimeSeries | 1D | 2D | 3D | 4D | 5D | 6D | 7D | 14D | 1M | 2M | 3M | 4M | 5M | 6M |
|---|---|---|---|---|---|---|---|---|---|---|---|---|---|---|
| **Panel A: No Input Variables** | | | | | | | | | | | | | | |
| Naive | 11.94 | 15.09 | 16.67 | 17.34 | 16.68 | 15.59 | 14.52 | **15.47** | **19.80** | **25.43** | **27.21** | **30.32** | **33.91** | **34.16** |
| Holt-Winters | **9.62** | **11.40** | **12.29** | **13.10** | **13.56** | **13.95** | 14.50 | 16.63 | 21.08 | 30.93 | 41.16 | 52.72 | 61.98 | 65.11 |
| AR(7) | 11.16 | 12.89 | 13.79 | 14.24 | 14.09 | 14.22 | **14.43** | 16.53 | 24.88 | 40.66 | 55.25 | 67.04 | 76.32 | 83.23 |
| **Panel B: With Actual Input Variables** | | | | | | | | | | | | | | |
| Model 1: AR(7)-L | 11.78 | 14.91 | 15.82 | 16.83 | 17.38 | 17.51 | 18.08 | 22.80 | 33.17 | 49.19 | 63.58 | 75.57 | 84.48 | 90.88 |
| Model 2: AR(7)-L-X | 11.53 | 15.03 | 16.22 | 17.01 | 17.31 | 16.58 | 16.17 | 21.89 | 35.20 | 52.98 | 65.11 | 72.83 | 77.64 | 80.62*** |
| Model 3: AR(7)-L-X-H | 9.39*** | 11.30*** | 12.35*** | 13.24** | 13.86 | 14.45 | 14.97 | 18.16 | 22.27*** | 28.43*** | 33.83*** | 39.81*** | 48.14*** | 56.37*** |
| Model 4: AR(7)-L-X-S | 9.35*** | 11.27*** | 12.36*** | 13.30* | 13.96 | 14.59 | 15.16 | 18.48 | 22.80*** | 29.03*** | 34.59*** | 40.76*** | 49.27*** | 57.71*** |
| Model 5: AR(7)-L-X-W | 9.38*** | 11.30*** | 12.40*** | 13.33* | 13.99 | 14.64 | 15.20 | 18.59 | 22.92*** | 29.11*** | 34.64*** | 40.70*** | 49.16*** | 57.51*** |
| Model 6: AR(7)-L-Seas/trend | 11.91 | 14.78 | 14.96 | 15.79 | 16.50 | 16.44 | 16.65 | 20.98 | 33.64 | 51.85 | 66.73 | 78.99 | 85.02 | 85.83 |
| Model 7: AR(7)-L-X-Seas/trend | 9.22*** | 10.72*** | 11.43*** | 12.19*** | 12.66*** | 13.11*** | 13.40*** | 15.37*** | 18.67*** | 23.68*** | 28.97*** | 35.40*** | 45.09*** | 54.96*** |
| Model 8: AR(7)-L-X-H-Seas/trend | 9.21*** | 10.66*** | 11.31*** | 12.01*** | 12.42*** | 12.82*** | 13.05*** | 14.88*** | 18.52*** | 23.82*** | 29.12*** | 35.52*** | 45.71*** | 55.35*** |
| Model 9: AR(7)-L-X-S-Seas/trend | **9.15**** | **10.59**** | **11.26**** | **11.98**** | **12.42**** | **12.81**** | **13.08**** | **14.85**** | **18.00**** | **23.03**** | **28.40**** | **35.04**** | **44.90**** | **54.89**** |
| Model 10: AR(7)-L-X-W-Seas/trend | 9.22*** | 10.71*** | 11.42*** | 12.17*** | 12.64*** | 13.09*** | 13.38*** | 15.34*** | 18.64*** | 23.66*** | 28.97*** | 35.42*** | 45.17*** | 55.12*** |
| **FFNN** | **1D** | **2D** | **3D** | **4D** | **5D** | **6D** | **7D** | **14D** | **1M** | **2M** | **3M** | **4M** | **5M** | **6M** |
| **Panel A: No Input Variables** | | | | | | | | | | | | | | |
| Naive | 11.94 | 15.09 | 16.67 | 17.34 | 16.68 | 15.59 | 14.52 | 15.47 | 19.80 | 25.43 | 27.21 | 30.32 | 33.91 | 34.16 |
| FFNNAR(7, 10, 5) | **10.43** | **12.31** | **13.16** | **13.53** | **13.98** | **13.90** | **14.00** | **15.36** | **19.19** | **22.03** | **23.69** | **26.01** | **26.20** | **25.34** |
| **Panel B: With Actual Input Variables** | | | | | | | | | | | | | | |
| Model 1: FFNNAR(7, 10, 5)-L | 10.29 | 12.03* | 12.99 | 13.51 | 13.76 | 14.18 | 14.68 | 16.96 | 22.29 | **24.59** | **25.41** | **26.21** | **26.79** | **28.16** |
| Model 2: FFNNAR(7, 10, 5)-L-X | 9.66*** | **11.16**** | 12.38** | 13.05 | 13.64 | 14.07 | 14.51 | **16.69** | **20.53** | 25.84 | 31.64 | 37.83 | 46.41 | 55.41 |
| Model 3: FFNNAR(7, 10, 5)-L-X-H | 9.94* | 11.79 | 12.76 | 13.43 | 14.20 | 14.35 | 15.21 | 18.42 | 22.31 | 27.93 | 33.22 | 38.77 | 47.09 | 56.04 |
| Model 4: FFNNAR(7, 10, 5)-L-X-S | **9.56*** | 11.19** | **12.07**** | **12.91*** | **13.30*** | **13.44** | **14.33** | 17.06 | 20.91 | 26.33 | 32.33 | 38.72 | 47.53 | 56.43 |
| Model 5: FFNNAR(7, 10, 5)-L-X-W | 9.72*** | 11.33*** | 12.20** | 12.96* | 13.76 | 13.95 | 14.56 | 17.30 | 21.22 | 26.66 | 32.08 | 38.12 | 46.66 | 55.17 |
| Model 6: FFNNAR(7, 10, 5)-L-Seas/trend | 11.18 | 13.17 | 15.68 | 15.68 | 17.61 | 18.50 | 18.48 | 26.43 | 52.88 | 63.97 | 75.22 | 86.87 | 110.77 | 117.68 |
| Model 7: FFNNAR(7, 10, 5)-L-X-Seas/trend | 9.86* | 11.78 | 12.88 | 13.79 | 14.77 | 16.04 | 16.72 | 22.14 | 26.88 | 31.86 | 36.35 | 40.11 | 48.19 | 56.69 |

(*continued on next page*)

**Table 7** (*continued*)

| Time Series | 1D | 2D | 3D | 4D | 5D | 6D | 7D | 14D | 1M | 2M | 3M | 4M | 5M | 6M |
|---|---|---|---|---|---|---|---|---|---|---|---|---|---|---|
| Model 8: FFNNAR(7, 10, 5)-L-X-H-Seas/trend | 10.60 | 12.56 | 13.60 | 15.27 | 16.40 | 17.31 | 18.30 | 25.05 | 31.22 | 36.38 | 39.63 | 44.92 | 51.93 | 56.61 |
| Model 9: FFNNAR(7, 10, 5)-L-X-S-Seas/trend | 10.19 | 11.69 | 13.17 | 14.04 | 14.80 | 15.49 | 16.23 | 20.71 | 28.59 | 29.66 | 34.22 | 39.56 | 48.58 | 56.26 |
| Model10: FFNNAR(7, 10, 5)-L-X-W-Seas/trend | 10.31 | 12.02 | 13.22 | 14.45 | 14.89 | 16.42 | 17.74 | 21.76 | 30.77 | 33.80 | 37.63 | 41.32 | 51.79 | 60.17 |

Notes: Bolded cells indicate forecasts with the highest accuracy for each horizon within individual panels, while grey-shaded cells highlight the most accurate forecasts for each horizon across the entire table. The variable L denotes load; X includes the weighted import price and natural gas price; and H, S, and W represent hydroelectric, solar PV, and onshore wind generation, respectively. The term *"Seas/trend"* refers to models incorporating Fourier terms, monthly dummy variables, and a linear time trend. Asterisks (***, **, *) indicate statistical significance at the 1 %, 5 %, and 10 % levels, respectively, based on the Diebold-Mariano test. In the *Time Series* section, the Diebold-Mariano test compares the RMSEs in Panel B to those from the AR (7) benchmark in Panel A. In the *FFNN* section, the test compares RMSEs in Panel B to those from the FFNNAR (7, 10, 5) benchmark in Panel A.

**Table 8**
MAPE for ex-ante forecasts of electricity prices in 2019.

| Time Series | 1D | 2D | 3D | 4D | 5D | 6D | 7D | 14D | 1M | 2M | 3M | 4M | 5M | 6M |
|---|---|---|---|---|---|---|---|---|---|---|---|---|---|---|
| **Panel A: No Input Variables** | | | | | | | | | | | | | | |
| Naive | 10.00 | 14.27 | 15.43 | 16.10 | 15.88 | 13.67 | 11.92 | 15.00 | 19.83 | 20.54 | 21.35 | 25.09 | 28.77 | 30.54 |
| Holt-Winters | **7.69** | **8.95** | **9.68** | **10.40** | **11.08** | **11.24** | **11.66** | **14.45** | **16.49** | **17.67** | 22.89 | 28.29 | 32.49 | 37.59 |
| AR(7) | 8.89 | 10.89 | 11.38 | 11.75 | 12.02 | 12.07 | 12.40 | 15.77 | 17.68 | 19.23 | **19.89** | **20.83** | **21.56** | **21.53** |
| **Panel B: With Actual Input Variables** | | | | | | | | | | | | | | |
| Model 1: AR(7)-L | **7.00** | **8.21** | **8.73** | **9.21** | **9.68** | **9.96** | **10.20** | **12.24** | 15.08 | 17.26 | 17.73 | 18.52 | 18.87 | **18.93** |
| Model 2: AR(7)-L-X | 7.11 | 8.45 | 9.08 | 9.74 | 10.22 | 10.47 | 10.84 | 13.08 | **14.47** | **15.01** | **15.37** | **16.30** | **18.06** | 19.28 |
| Model 3: AR(7)-L-X-H | 7.52 | 9.37 | 10.18 | 11.08 | 11.97 | 12.59 | 13.07 | 16.85 | 20.87 | 23.13 | 24.05 | 25.15 | 26.36 | 27.53 |
| Model 4: AR(7)-L-X-S | 7.11 | 8.58 | 9.33 | 10.01 | 10.55 | 10.90 | 11.30 | 13.91 | 15.82 | 17.16 | 18.31 | 19.64 | 21.58 | 22.81 |
| Model 5: AR(7)-L-X-W | 7.12 | 8.60 | 9.35 | 10.03 | 10.54 | 10.88 | 11.27 | 13.74 | 15.57 | 16.96 | 18.16 | 19.55 | 21.48 | 22.66 |
| Model 6: AR(7)-L-Seas/trend | 7.21 | 8.90 | 9.79 | 10.46 | 11.25 | 11.67 | 12.16 | 15.47 | 20.44 | 25.52 | 28.44 | 31.02 | 33.61 | 35.41 |
| Model 7: AR(7)-L-X-Seas/trend | 7.39 | 9.08 | 9.91 | 10.79 | 11.40 | 11.98 | 12.50 | 15.77 | 18.85 | 20.93 | 22.11 | 23.21 | 24.89 | 25.90 |
| Model 8: AR(7)-L-X-H-Seas/trend | 7.47 | 9.42 | 10.31 | 11.36 | 12.28 | 12.95 | 13.47 | 17.58 | 22.14 | 25.04 | 25.71 | 26.58 | 27.74 | 29.01 |
| Model 9: AR(7)-L-X-S-Seas/trend | 7.39 | 9.05 | 9.88 | 10.77 | 11.42 | 12.00 | 12.55 | 15.94 | 19.16 | 21.23 | 22.37 | 23.35 | 25.01 | 26.07 |
| Model 10: AR(7)-L-X-W-Seas/trend | 7.39 | 9.09 | 9.92 | 10.80 | 11.40 | 11.99 | 12.52 | 15.76 | 18.84 | 20.91 | 22.09 | 23.17 | 24.81 | 25.80 |
| **FFNN** | **1D** | **2D** | **3D** | **4D** | **5D** | **6D** | **7D** | **14D** | **1M** | **2M** | **3M** | **4M** | **5M** | **6M** |
| **Panel A: No Input Variables** | | | | | | | | | | | | | | |
| Naive | 10.00 | 14.27 | 15.43 | 16.10 | 15.88 | 13.67 | 11.92 | **15.00** | **19.83** | **20.54** | **21.35** | **25.09** | **28.77** | **30.54** |
| FFNNAR(7, 10, 20) | **9.08** | **10.55** | **11.22** | **11.57** | **11.46** | **11.32** | **11.78** | 15.31 | 20.86 | 30.62 | 43.20 | 49.89 | 59.78 | 62.55 |
| **Panel B: With Actual Input Variables** | | | | | | | | | | | | | | |
| Model 1: FFNNAR(7, 10, 20)-L | **8.27** | 10.14 | **10.63** | 11.37 | 11.92 | 12.28 | 13.30 | 16.72 | 21.46 | 25.91 | 27.19 | 30.68 | 33.81 | 35.44 |
| Model 2: FFNNAR(7, 10, 20)-L-X | 8.50 | 10.43 | 10.79 | 11.19 | 11.73 | 11.79 | 12.52 | 15.97 | 18.82 | 19.94 | 21.32 | 22.78 | 23.74 | 24.93 |
| Model 3: FFNNAR(7, 10, 20)-L-X-H | 8.40 | 10.16 | 11.07 | 11.78 | 12.21 | 12.31 | 13.46 | 19.56 | 24.36 | 27.78 | 29.04 | 28.23 | 27.22 | 25.99 |
| Model 4: FFNNAR(7, 10, 20)-L-X-S | 8.47 | 10.01 | 10.84 | **11.16** | **11.56** | **11.72** | **12.34** | **15.43** | 19.16 | 20.72 | 21.09 | 22.41 | 23.69 | 25.79 |
| Model 5: FFNNAR(7, 10, 20)-L-X-W | 8.41 | 9.99 | 10.75 | 11.41 | 11.70 | 12.05 | 12.77 | 15.73 | **18.58** | 19.87 | **20.87** | **21.81** | **23.70** | 25.04 |
| Model 6: FFNNAR(7, 10, 20)-L-Seas/trend | 8.70 | 10.52 | 11.13 | 11.56 | 12.57 | 12.96 | 13.72 | 17.60 | 21.62 | 23.72 | 24.98 | 27.38 | 27.42 | 27.07 |
| Model 7: FFNNAR(7, 10, 20)-L-X-Seas/trend | 8.45 | 9.78 | 10.88 | 11.30 | 12.10 | 12.57 | 12.76 | 15.75 | 19.65 | 20.98 | 21.46 | 22.36 | 24.23 | **24.46** |
| Model 8: FFNNAR(7, 10, 20)-L-X-H-Seas/trend | 8.37 | **9.77** | 10.72 | 11.21 | 11.92 | 12.45 | 12.94 | 15.71 | 19.10 | **19.86** | 21.05 | 21.88 | 23.73 | 24.92 |
| Model 9: FFNNAR(7, 10, 20)-L-X-S-Seas/trend | 8.52 | 9.84 | 11.01 | 11.65 | 11.86 | 12.33 | 12.47 | 15.77 | 19.49 | 21.06 | 21.83 | 22.77 | 24.11 | 25.12 |
| Model10:FFNNAR(7, 10, 20)-L-X-W-Seas/trend | 8.44 | 9.89 | 10.94 | 11.74 | 12.11 | 12.53 | 13.49 | 16.53 | 19.60 | 20.75 | 21.73 | 22.35 | 23.96 | 24.83 |

Notes: Bolded cells indicate forecasts with the highest accuracy for each horizon within individual panels, while grey-shaded cells highlight the most accurate forecasts for each horizon across the entire table. The variable L denotes load; X includes the weighted import price and natural gas price; and H, S, and W represent hydroelectric, solar PV, and onshore wind generation, respectively. The term *"Seas/trend"* refers to models incorporating Fourier terms, monthly dummy variables, and a linear time trend.

**Table 9**
MAPE for ex-ante forecasts of electricity prices in 2024.

| Time Series | 1D | 2D | 3D | 4D | 5D | 6D | 7D | 14D | 1M | 2M | 3M | 4M | 5M | 6M |
|---|---|---|---|---|---|---|---|---|---|---|---|---|---|---|
| Panel A: No Input Variables | | | | | | | | | | | | | | |
| Naive | 8.41 | 11.01 | 12.32 | 12.93 | 12.39 | 11.44 | 10.39 | **11.06** | **15.01** | **19.14** | **21.68** | **24.33** | **26.99** | **27.35** |
| Holt-Winters | **6.96** | **8.16** | **8.80** | **9.29** | **9.34** | **9.82** | **10.33** | 11.76 | 15.14 | 23.32 | 32.31 | 39.38 | 45.73 | 49.43 |
| AR(7) | 8.13 | 9.44 | 10.24 | 10.69 | 10.51 | 10.54 | 10.70 | 13.13 | 20.55 | 33.94 | 47.35 | 59.34 | 69.97 | 78.01 |
| **Panel B: With Actual Input Variables** | | | | | | | | | | | | | | |
| Model 1: AR(7)-L | 9.15 | 11.47 | 11.95 | 12.84 | 13.24 | 13.38 | 13.96 | 17.80 | 25.97 | 39.84 | 54.14 | 67.04 | 76.31 | 83.85 |
| Model 2: AR(7)-L-X | 8.76 | 11.60 | 12.27 | 12.98 | 13.27 | 13.01 | 13.17 | 18.18 | 29.46 | 45.52 | 57.33 | 65.52 | 70.81 | 74.51 |
| Model 3: AR(7)-L-X-H | 7.00 | 8.63 | 9.44 | 10.13 | 10.85 | 11.66 | 12.33 | 14.92 | 18.00 | 22.55 | 27.21 | 32.43 | 39.32 | 46.47 |
| Model 4: AR(7)-L-X-S | 6.99 | 8.64 | 9.46 | 10.24 | 10.97 | 11.77 | 12.49 | 15.14 | 18.30 | 22.78 | 27.45 | 32.85 | 39.82 | 47.13 |
| Model 5: AR(7)-L-X-W | 7.01 | 8.64 | 9.49 | 10.24 | 10.98 | 11.83 | 12.53 | 15.22 | 18.47 | 22.93 | 27.65 | 32.97 | 39.95 | 47.22 |
| Model 6: AR(7)-L-Seas/trend | 9.36 | 11.15 | 11.18 | 11.61 | 12.07 | 11.95 | 11.93 | 15.23 | 25.25 | 39.03 | 48.82 | 55.92 | 61.34 | 65.74 |
| Model 7: AR(7)-L-X-Seas/trend | 6.89 | 8.07 | 8.67 | 9.24 | 9.61 | 10.09 | 10.57 | 12.13 | 14.69 | 18.88 | 23.24 | 29.05 | 37.24 | 45.75 |
| Model 8: AR(7)-L-X-H-Seas/trend | 6.90 | 8.02 | 8.58 | 9.11 | 9.46 | 9.84 | **10.26** | 11.75 | 14.50 | 19.05 | 23.56 | 29.41 | 37.86 | 46.18 |
| Model 9: AR(7)-L-X-S-Seas/trend | **6.85** | **7.98** | **8.52** | **9.07** | **9.41** | **9.81** | 10.27 | **11.74** | **14.19** | **18.33** | **22.54** | **28.63** | **36.89** | **45.61** |
| Model 10: AR(7)-L-X-W-Seas/trend | 6.89 | 8.06 | 8.65 | 9.22 | 9.60 | 10.08 | 10.56 | 12.12 | 14.67 | 18.86 | 23.21 | 29.07 | 37.29 | 45.88 |
| **FFNN** | **1D** | **2D** | **3D** | **4D** | **5D** | **6D** | **7D** | **14D** | **1M** | **2M** | **3M** | **4M** | **5M** | **6M** |
| **Panel A: No Input Variables** | | | | | | | | | | | | | | |
| Naive | 8.41 | 11.01 | 12.32 | 12.93 | 12.39 | 11.44 | 10.39 | **11.06** | 15.01 | 19.14 | 21.68 | 24.33 | 26.99 | 27.35 |
| FFNNAR(7, 10, 5) | **7.85** | **9.17** | **9.88** | **10.12** | **10.35** | **10.26** | **10.35** | 11.77 | **14.44** | **16.68** | **18.28** | **19.20** | **18.91** | **17.95** |
| **Panel B: With Actual Input Variables** | | | | | | | | | | | | | | |
| Model 1: FFNNAR(7, 10, 5)-L | 7.82 | 9.17 | 9.86 | 10.20 | 10.42 | 10.69 | 11.27 | 13.83 | 17.74 | **19.15** | **20.02** | **20.79** | **21.50** | **22.81** |
| Model 2: FFNNAR(7, 10, 5)-L-X | 7.24 | 8.47 | 9.36 | 9.86 | 10.42 | 10.70 | 11.06 | **12.79** | **15.74** | 20.19 | 25.16 | 30.70 | 37.62 | 45.69 |
| Model 3: FFNNAR(7, 10, 5)-L-X-H | 7.47 | 8.82 | 9.71 | 10.32 | 11.01 | 11.17 | 11.82 | 14.84 | 17.85 | 21.96 | 26.52 | 31.34 | 37.91 | 45.60 |
| Model 4: FFNNAR(7, 10, 5)-L-X-S | **7.05** | **8.02** | **8.80** | **9.47** | **9.95** | **10.10** | **10.71** | 13.03 | 16.02 | 20.32 | 25.49 | 31.11 | 38.29 | 46.39 |
| Model 5: FFNNAR(7, 10, 5)-L-X-W | 7.26 | 8.45 | 9.13 | 9.70 | 10.32 | 10.57 | 11.16 | 13.12 | 16.22 | 20.75 | 25.43 | 30.90 | 38.00 | 45.54 |
| Model 6: FFNNAR(7, 10, 5)-L-Seas/trend | 8.22 | 9.66 | 11.78 | 11.55 | 12.81 | 13.10 | 14.00 | 19.63 | 31.92 | 37.48 | 44.22 | 48.09 | 56.36 | 61.62 |
| Model 7: FFNNAR(7, 10, 5)-L-X-Seas/trend | 7.52 | 8.83 | 9.49 | 10.30 | 11.16 | 12.28 | 13.25 | 17.09 | 20.97 | 25.38 | 30.11 | 33.27 | 39.90 | 46.33 |
| Model 8: FFNNAR(7, 10, 5)-L-X-H-Seas/trend | 8.11 | 9.42 | 10.36 | 11.60 | 12.75 | 13.56 | 14.51 | 19.23 | 25.02 | 29.53 | 32.31 | 37.32 | 42.70 | 46.53 |
| Model 9: FFNNAR(7, 10, 5)-L-X-S-Seas/trend | 7.76 | 8.72 | 9.73 | 10.50 | 11.16 | 11.88 | 12.63 | 15.71 | 21.38 | 23.76 | 27.56 | 32.52 | 38.78 | 45.31 |
| Model10: FFNNAR(7, 10, 5)-L-X-W-Seas/trend | 7.78 | 8.99 | 9.78 | 10.62 | 11.41 | 12.65 | 13.93 | 16.94 | 23.41 | 26.44 | 31.04 | 34.24 | 42.40 | 48.77 |

Notes: Bolded cells indicate forecasts with the highest accuracy for each horizon within individual panels, while grey-shaded cells highlight the most accurate forecasts for each horizon across the entire table. The variable L denotes load; X includes the weighted import price and natural gas price; and H, S, and W represent hydroelectric, solar PV, and onshore wind generation, respectively. The term *"Seas/trend"* refers to models incorporating Fourier terms, monthly dummy variables, and a linear time trend.

the sense that future data for input variables is unavailable, particularly for forecast horizons extending beyond one-day. To address this limitation, we forecast the input variables, and for the next stage of analysis, we replace the actual input data with forecasted values for the test and forecast period. We develop forecasting models for load, weighted import prices, natural gas prices, and RES.

Beginning with the load forecasting process, the literature indicates a V-shaped relationship between load and temperature (Behmiri et al., 2023). Our data shows that this relationship exhibits a negative association at lower temperatures and a positive one at higher levels, with the turning point occurring at approximately 60 °F (15.6 °C). Additionally, the slope of the relationship is asymmetric, with a steeper slope observed during warmer seasons. Based on the approach of Fezzi and Fanghella (2021), we incorporate asymmetry into the relationship by employing a linear spline function. The function is defined with a knot at the minimum load, which we set at 60 °F. Furthermore, we include Fourier terms to capture annual cycles, dummy variables for days of the week, and a separate dummy variable for national holidays. We use Model 11 for load forecasting, spanning from one day to six months ahead, which is an ***ARMAX*** (1,1) model as follows:

$$y_t = \beta_0 + \phi_1 y_{t-1} + \boldsymbol{D_t}'\varphi + \beta_1 T_t + \beta_2 d_{60}(T_t - 60) + A + \psi_1 \varepsilon_{t-1} + \varepsilon_t \tag{11}$$

where $y_t$ is the load at time $t$, and $\boldsymbol{D_t}'$ includes the vector of dummy variables for Saturdays, Sundays, Mondays, and national holidays. These days are considered periods with the least demand, as during the weekends, many economic activities are suspended and, therefore, the electricity load significantly decreases. While Monday is characterized by a quicker increase in demand compared to the other weekdays, the demand is less than other days (Pardo et al., 2002). We incorporate the drop in demand during public holidays by including an additional binary variable (Pardo et al., 2002; Hong et al., 2014). $T_t$ is the Milan average daily temperature at time $t$, and $d_{60}$ is a binary variable equal to 1 if the temperature is higher than or equal to 60 °F and zero otherwise. Furthermore, $A$ denotes the Fourier terms capturing recurring seasonal patterns of annual cycles in electricity prices.

We utilize the climatology method, which involves using the average temperature of the same date over the past 5 years as the forecasted temperature (Hu et al., 2015; Behmiri et al., 2023). Other variables and symbols are defined as previously stated.

In order to forecast the weighted import price, incorporating weekly Fourier terms yield superior performance. Therefore, in Model 12, we adopt the following specification:

$$y_t = \beta_0 + \phi_1 y_{t-1} + F + \varepsilon_t \tag{12}$$

where $y_t$ represents the weighted import price at time $t$, $F$ includes the Fourier terms accounting for the weekly cycles defined previously, and all other symbols are as before.

In forecasting RES, incorporating both weekly and yearly seasonality using Fourier terms leads to improved performance. Therefore, for hydroelectric, wind, and solar generations, we employ Model 13:

$$y_t = \beta_0 + \phi_1 y_{t-1} + F + A + \varepsilon_t \tag{13}$$

where $y_t$ represents hydroelectric, wind and solar generation at time $t$ (each RES is represented by a separate model). All other variables and symbols are as previously defined. Furthermore, we use the naïve method to forecast natural gas prices from one-day to six-months ahead.

The RMSE results for this set of forecasts for the years 2019 and 2024 are presented in Tables 6 and 7, respectively, while the corresponding MAPE values are reported in Tables 8 and 9.

There is an overall rise in RMSE and MAPE values across both 2019 and 2024, demonstrating a decline in forecast accuracy compared to the ex-post forecasts that utilize actual data. This confirms that forecasting errors in the input variables introduce additional uncertainty into electricity price predictions.

In 2019, the time series Model 1 (which includes load), and Model 2 (which incorporates load, natural gas prices, and weighted imports) steadily outperformed all other specifications, including *FFNN* models, across all forecast horizons. There is no evidence that renewable energy sources contributed predictive value to electricity price forecasting during this period using forecasted data.

In 2024, the time series Models 3 to 5, which includes RES, consistently outperformed Model 2 across all horizons. Additionally, Models 8 to 10, which combine renewables with seasonality and trend components, yielded the strongest forecasting performance, particularly for horizons up to one month ahead. However, for longer horizons from two- to six-months the *FFNNAR*(7, 10, 5) model without input variables demonstrated more competitive performance. Therefore, the inclusion of renewable generation variables still adds some predictive value, particularly solar generation, as solar availability is relatively straightforward to forecast. Hydropower, which indicated increasing predictive power in the ex-post 2024 models, contributes less to the ex-ante forecasts, likely due to the lack of accurate hydropower generation forecasts. The MAPE results, reported in Tables 8 and 9, largely confirm the findings observed in the RMSE analysis.

We conducted several additional analyses. First, we estimated models without autoregressive terms, and we found that models including seven lagged prices outperformed those without them across all forecast horizons. Second, we examined the goodness-of-fits across the four seasons, Spring, Summer, Autumn, and Winter, and the conclusions were consistent with the main findings. Third, we explored alternative methods for forecasting input variables, such as using data from the same date in the previous year or using moving averages of historical values. However, the initial forecasts based on the autoregressive models (Models 11–13) yielded more accurate results for all horizons.

Additionally, we conducted estimations by including crude oil, coal, and $\boldsymbol{CO_2}$ emission prices in our models, but found no advantage, particularly for mid-term horizons. Furthermore, we attempted to forecast by integrating all three RES into a single model.

However, this approach resulted in a decline in forecasting performance compared to the results obtained when each RES was included separately.

Finally, we applied one of the expert models suggested by Ziel and Weron (2018), as implemented by Billé et al. (2023), modified to fit daily data. In this model, electricity prices are explained by the mean value of prices over the last seven days ($\bar{y}_t$) and eight autoregressive terms ($k = 1, \ldots, 8$) that are demeaned with respect to $\bar{y}_t$ as ($\sum_{k=1}^{8} (y_{t-k} - \bar{y}_t)$). We extended this model by including the same variables as Models 1–10. However, these extensions did not result in persistently higher forecasting accuracy. The original expert model is designed for hourly data and short-term forecasting, so our extension to daily data and mid-term forecasting might require additional structure. We leave the investigating of this aspect to future research.

## 7. Concluding remarks

Forecasting electricity prices is a challenging task due to several inherent characteristics. One key factor is that electricity is non-storable, which necessitates a continuous equilibrium between production and consumption to maintain system stability. Hence, electricity market price exhibits substantial variability, calendar seasonality mirroring demand patterns, unexpected and short spikes, nonlinearity, and heteroscedasticity. Furthermore, the rapid and widespread increase of renewable sources has significant consequences on the electricity supply side, adding complexity to the modelling and forecasting of prices. Therefore, energy market studies dealing with future time horizons must develop forecasting models that explicitly account for the dynamic patterns of renewable generation.

Motivated by the above issues, we developed models to forecast electricity prices which, in addition to information on load and input prices, also include data on renewable energy production. These models enable an investigation into the influence of these factors in forecasting electricity prices in Northern Italy, a region with a significant share of renewable production.

This study evaluated a range of models, including linear time-series models and feedforward neural networks, to predict daily electricity prices across short- to medium-term horizons. The analysis relies on actual data for the input variables during the estimation phase and is subsequently extended by incorporating forecasted input values to develop realistic ex-ante forecasting scenarios. Forecasting results are reported for the years 2019 and 2024. This comparison allows us to assess the contribution of renewable energy sources, given that their share in the electricity mix increased significantly between these two periods.

The results indicate that in 2019, conventional time series models incorporating load, natural gas prices, and imports outperformed the benchmarks, while renewable energy sources, especially hydropower, offered limited additional predictive power. By 2024, however, the predictive power of renewable energy sources, particularly hydropower, increased due to their growing share in the electricity mix. Despite this, overall forecasting accuracy declined in 2024 across all horizons, reflecting higher market volatility and the challenges partially introduced by greater renewable energy penetration. In contrast to 2019, feedforward neural networks outperformed time series models in 2024, owing to their ability to model complex, nonlinear relationships.

Using forecasted input variables for the testing and forecasting periods (ex-ante forecasts) highlights the crucial role of accurate input predictions. While the time series models using forecasted load and cost variables remained dominant in 2019, the inclusion of renewable energy sources, especially solar, marginally improved forecasts in 2024. Nevertheless, the value of renewable energy sources in ex-ante models is conditional on the quality of their own forecasts.

Our findings suggest that incorporating renewable energy variables has become more critical in recent years, as their contribution to price changes is no longer marginal. The increasing share of renewable energy sources across Europe, driven by policy targets and technological innovations, has made electricity markets more weather-dependent and volatile. This shift emphasizes the necessity of integrating renewable energy sources into price forecasting models. At the same time, the decline in the overall accuracy of price forecasting indicates the need to improve forecasting tools to handle the increased uncertainty associated with higher shares of renewables. These findings emphasize the need for data-driven models, particularly machine learning approaches, as electricity markets become more complex.

The findings have implications for both market participants and policymakers. Market participants, including traders, retailers, and generators operating in short- and medium-term electricity markets, rely heavily on price forecasts to inform bidding strategies, risk management, and dispatch decisions. Improved forecasting accuracy, as demonstrated in our study by including renewable energy generation, can improve hedging efficiency by supporting more accurate positions in forward markets. While the predictive gain from adding renewable energy sources may seem marginal, as Xu (2004) suggested, their economic impact can be substantial when used in dynamic trading strategies. This supports the view that even modest forecasting power can lead to significant economic gains under realistic assumptions. Therefore, a marginal reduction in the RMSE can lead to lower imbalance costs, better contract pricing, and improved profitability in trading strategies. This is particularly relevant in contemporary electricity markets characterized by increasing uncertainty.

For policymakers and regulators, the findings highlight the importance of ensuring transparency and availability of high-quality, real-time data on renewable energy generation. Such transparency is essential for forecasts to remain useful for market participants and effective for grid planning.

Although this study focuses on the Northern Italian market, the results are expected to be generalizable to the broader Italian electricity market and to other European markets experiencing similar transitions towards renewable energy sources. Many European countries are rapidly increasing their renewable energy capacity, facing similar challenges of price volatility caused by intermittency, and fundamental shifts in market dynamics. Consequently, the conclusions of this study are expected to hold for other liberalized and decarbonizing electricity markets across Europe.

## CRediT authorship contribution statement

**Niaz Bashiri Behmiri:** Writing – review & editing, Writing – original draft, Software, Methodology, Formal analysis, Data curation, Conceptualization. **Carlo Fezzi:** Writing – review & editing, Supervision, Funding acquisition. **Francesco Ravazzolo:** Writing – review & editing, Supervision, Funding acquisition.

## Declaration of generative AI and AI-assisted technologies in the writing process

During the preparation of this work the authors used ChatGPT in order to improve readability of the manuscript. After using this tool/service, the authors reviewed and edited the content as needed and took full responsibility for the content of the publication.

## Declaration of competing interest

The authors declare that they have no known competing financial interests or personal relationships that could have appeared to influence the work reported in this paper.

## Acknowledgement

We acknowledge financial support from the Province of Bolzano-Bozen under the project SHE -Seasonal Hydrological Econometric Forecasting for Hydropower Optimization (grant E62F20000130003). We thank the conference participants at the 17th IAEE European Energy Conference, The Future of Global Energy System.

## Data availability

Data will be made available on request.

## References

Andreas, Z., 1994. In: Simulation Neuronaler Netze [Simulation of Neural Network], first ed., 73. Addison-Wesley (in German) ISBN 3-89319-554-8.
Antweiler, W., Muesgens, F., 2021. On the long-term merit order effect of renewable energies. Energy Econ. 99, 105275.
Behm, C., Nolting, L., Praktiknjo, A., 2020. How to model European electricity load profiles using artificial neural networks. Appl. Energy 277, 115564.
Behmiri, N.B., Fezzi, C., Ravazzol, F., 2023. Incorporating air temperature into mid-term electricity load forecasting models using time-series regressions and neural networks. Energy 278, 127831.
Belenguer, E., Segarra-Tamarit, J., Pérez, E., Vidal-Albalate, R., 2025. Short-term electricity price forecasting through demand and renewable generation prediction. Math. Comput. Simulat. 229, 350–361.
Bernardi, M., Lisi, F., 2020. Point and interval forecasting of zonal electricity prices and demand using heteroscedastic models: the IPEX case. Energies 13 (23), 6191.
Bigerna, S., 2018. Estimating temperature effects on the Italian electricity market. Energy Policy 118, 257–269.
Billé, A.G., Gianfreda, A., Del Grosso, F., Ravazzolo, F., 2023. Forecasting electricity prices with expert, linear, and nonlinear models. Int. J. Forecast. 39 (2), 570–586.
Bonato, M., Ranzani, A., Patro, E.R., Gaudard, L., De Michele, C., 2019. Water-energy nexus for an Italian storage hydropower plant under multiple drivers. Water 11, 1–25.
Busse, J., Rieck, J., 2022. Mid-term energy cost-oriented flow shop scheduling: integration of electricity price forecasts, modeling, and solution procedures. Comput. Ind. Eng. 163, 107810.
Catalao, J.P.S., Mariano, S.J.P.S., Mendes, V.M.F., Ferreira, L.A.F.M., 2007. Short-term electricity prices forecasting in a competitive market: a neural network approach. Elec. Power Syst. Res. 77, 1297–1304.
Cheng, H., Ding, X., Zhou, W., Ding, R., 2019. A hybrid electricity price forecasting model with Bayesian optimization for German energy exchange. Electrical Power and Energy Systems 110, 653–666.
Ciarreta, A., Martinez, B., Nasirov, S., 2023. Forecasting Electricity Prices Using Bid Data. International Journal of Forecasting, forthcoming.
Diebold, F., Mariano, R., 1995. Comparing predictive accuracy. J. Bus. Econ. Stat. 13, 253–263.
Engelbrecht, A.P., 2007. Computational Intelligence: an Introduction, second ed. Wiley, Hoboken.
Escribano, A., Pena, J.I., Villaplana, P., 2011. Modelling electricity prices: international evidence. Oxf. Bull. Econ. Stat. 73 (5), 622–650.
Fezzi, C., Bunn, D., 2010. Structural analysis of electricity demand and supply interactions. Oxf. Bull. Econ. Stat. 72 (6), 827–856.
Fezzi, C., Fanghella, V., 2021. Tracking GDP in real-time using electricity market data: insights from the first wave of COVID-19 across Europe. Eur. Econ. Rev. 139, 103907.
Fezzi, C., Mosetti, L., 2020. Size matters: estimation sample length and electricity price forecasting accuracy. Energy J. 41, 231–254.
Fletcher, R., 1987. Practical methods of optimization, 2nd Edition. John Wiley and Sons, Chichester.
Foroni, C., Ravazzolo, F., Rossini, L., 2023. Are low frequency macroeconomic variables important for high frequency electricity prices? Econ. Modell. 120, 106160.
Ghelasi, P., Ziel, F., 2023. Hierarchical forecasting for aggregated curves with an application to day-ahead electricity price auctions. Int. J. Forecast. forthcoming.
Ghelasi, P., Ziel, F., 2025. From day-ahead to mid and long-term horizons with econometric electricity price forecasting models. Renew. Sustain. Energy Rev. 217, 115684.
Gianfreda, A., Parisio, L., Pelagatti, M., 2018. A review of balancing costs in Italy before and after RES introduction. BEMPS-Bozen Economics and Management paper series 45.
Gianfreda, A., Ravazzolo, F., Rossini, L., 2020. Comparing the forecasting performances of linear models for electricity prices with high-RES penetration. Int. J. Forecast. 36 (3), 974–986.
Gianfreda, A., Ravazzolo, F., Rossini, L., 2023. Large time-varying volatility models for hourly electricity prices. Oxf. Bull. Econ. Stat. 85, 305–9049.
Gürtler, M., Paulsen, T., 2018. The effect of wind and solar power forecasts on day-ahead and intraday electricity prices in Germany. Energy Econ. 75, 150–162.
Haugom, E., Ullrich, C.J., 2012. Forecasting spot price volatility using the short-term forward curve. Energy Econ. 34, 1826–1833.
Holt, C.C., 1957. Forecasting Seasonals and Trends by Exponentially Weighted Averages. Carnegie Institute of Technology, Pittsburgh USA.
Hong, T., Pinson, P., Fan, S., 2014. Global energy forecasting competition 2012. Int. J. Forecast. 30, 357–363.
Hu, Z., Bao, Y., Chiong, R., Xiong, T., 2015. Mid-term interval load forecasting using multi-output support vector regression with a memetic algorithm for feature selection. Energy 84, 419–431.

Hyndman, R., Athanasopoulos, G., Bergmeir, C., Caceres, G., Chhay, L., O'Hara-Wild, M., Petropoulos, F., Razbash, S., Wang, E., Yasmeen, F., et al., 2020. Package 'Forecast': Forecasting Functions for Time Series and Linear Models.
Jiang, P., Nie, Y., Wang, J., Huang, X., 2023. Multivariable short-term electricity price forecasting using artificial intelligence and multi-input multi-output scheme. Energy Econ. 117, 106471.
Kaminski, V., 2013. Energy Markets. Risk Books.
Lago, J., Marcjasz, G., De Schutter, B., Weron, R., 2021. Forecasting day-ahead electricity prices: a review of state-of-the-art algorithms, best practices and an open-access benchmark. Appl. Energy 293, 116983.
Lehna, M., Scheller, F., Herwartz, H., 2022. Forecasting day-ahead electricity prices: a comparison of time series and neural network models taking external regressors into account. Energy Econ. 106, 105742.
Li, W., Becker, D.M., 2021. Day-ahead electricity price prediction applying hybrid models of LSTM-based deep learning methods and feature selection algorithms under consideration of market coupling. Energy 237, 121543.
Maciejowsk, K., Nowotarski, J., Weron, R., 2016. Probabilistic forecasting of electricity spot prices using Factor Quantile regression averaging. Int. J. Forecast. 32 (3), 957–965.
Maciejowska, M., Nitka, W., Weron, T., 2021. Enhancing load, wind and solar generation for day-ahead forecasting of electricity prices. Energy Econ. 99, 105273.
Marcjasz, G., Uniejewski, B., Weron, R., 2019. On the importance of the long-term seasonal component in day-ahead electricity price forecasting with NARX neural networks. Int. J. Forecast. 35, 1520–1532.
Monjazeb, M.R., Amiri, H., Movahedi, A., 2024. Wholesale electricity price forecasting by Quantile regression and Kalman filter method. Energy 290, 129925.
Muniain, P., Ziel, F., 2020. Probabilistic forecasting in day-ahead electricity markets: simulating peak and off-peak prices. Int. J. Forecast. 36, 1193–1210.
Nowotarski, J., Weron, R., 2016. On the importance of the long-term seasonal component in day-ahead electricity price forecasting. Energy Econ. 57, 228–235.
Olivares, K.G., Challu, C., Marcjasz, G., Weron, R., Dubrawski, A., 2023. Neural basis expansion analysis with exogenous variables: forecasting electricity prices with NBEATSx. Int. J. Forecast. 39 (2), 884–900.
Pardo, A., Meneu, V., Valor, E., 2002. Temperature and seasonality influences on Spanish electricity load. Energy Econ. 24, 55–70.
Poggi, A., Persio, L.D., Ehrhard, M., 2023. Electricity price forecasting via statistical and deep learning approaches: the German case. AppliedMath 3 (2), 316–342.
Revelle, W., 2016. Psych: Procedures for Personality and Psychological Research. Northwestern University, Evanston, Illinois, USA.
Shah, I., Lisi, F., 2019. Forecasting of electricity price through a functional prediction of sale and purchase curves. J. Forecast. 39, 242–259.
Shao, Z., Yang, Y., Zheng, O., Zhou, K., Liu, C., Yang, S., 2022. A pattern classification methodology for interval forecasts of short-term electricity prices based on hybrid deep neural networks: a comparative analysis. Appl. Energy 327, 120115.
Shi, W., Wang, Y., Chen, Y., Ma, Y., 2021. An effective two-stage electricity price forecasting scheme. Elec. Power Syst. Res. 199, 107416.
Steinert, R., Ziel, F., 2019. Short- to mid-term day-ahead electricity price forecasting using futures. Energy J. 40 (1), 105–128.
Sulandari, W., Subanar, S., Lee, M.H., Rodrigues, P.C., 2020. Indonesian electricity load forecasting using singular spectrum analysis, fuzzy systems and neural network. Energy 190, 116408.
Uniejewski, B., Marcjasz, G., Weron, R., 2019. Understanding intraday electricity markets: variable selection and very short-term price forecasting using LASSO. Int. J. Forecast. 35, 1533–1547.
Uniejewski, B., Maciejowska, K., 2023. LASSO principal component averaging: a fully automated approach for point forecast pooling. Int. J. Forecast. 39 (4), 1839–1852.
Wagner, A., Ramentol, E., Schirra, F., Michaeli, H., 2022. Short- and long-term forecasting of electricity prices using embedding of calendar information in neural networks. Journal of Commodity Markets 28, 100246.
Winters, P.R., 1960. Forecasting sales by exponentially weighted moving averages. Manag. Sci. 6 (3), 324–342.
Weron, R., Misiorek, A., 2008. Forecasting spot electricity prices: a comparison of parametric and semiparametric time series models. Int. J. Forecast. 24, 744–763.
Weron, R., 2014. Electricity price forecasting: a review of the state-of-the-art with a look into the future. Int. J. Forecast. 30, 1030–1081.
Xu, Y., 2004. Small levels of predictability and large economic gains. J. Empir. Finance 11, 247–275.
Yang, Z., Ce, L., Lian, L., 2017. Electricity price forecasting by a hybrid model, combining wavelet transform, ARMA and kernel-based extreme learning machine methods. Appl. Energy 190, 291–305.
Ziel, F., Steinert, R., 2018. Probabilistic mid- and long-term electricity price forecasting. Renew. Sustain. Energy Rev. 94, 251–266.
Ziel, F., Weron, R., 2018. Day-ahead electricity price forecasting with high-dimensional structures: univariate vs. multivariate modeling frameworks. Energy Econ. 70, 396–420.